INFORMATION TO USERS

This manuscript has been reproduced from the microfilm master. UMI films the text directly from the original or copy submitted. Thus, some thesis and dissertation copies are in typewriter face, while others may be from any type of computer printer.

The quality of this reproduction is dependent upon the quality of the copy submitted. Broken or indistinct print, colored or poor quality illustrations and photographs, print bleedthrough, substandard margins, and improper alignment can adversely affect reproduction.

In the unlikely event that the author did not send UMI a complete manuscript and there are missing pages, these will be noted. Also, if unauthorized copyright material had to be removed, a note will indicate the deletion.

Oversize materials (e.g., maps, drawings, charts) are reproduced by sectioning the original, beginning at the upper left-hand corner and continuing from left to right in equal sections with small overlaps. Each original is also photographed in one exposure and is included in reduced form at the back of the book.

Photographs included in the original manuscript have been reproduced xerographically in this copy. Higher quality 6" x 9" black and white photographic prints are available for any photographs or illustrations appearing in this copy for an additional charge. Contact UMI directly to order.

UMI

A Bell & Howell Information Company
300 North Zeeb Road, Ann Arbor MI 48106-1346 USA
313/761-4700 800/521-0600

CHARACTERIZATION OF INTERSTITIAL ABNORMALITIES IN NATURALLY OCCURRING RENAL DISEASE IN DOGS

A thesis

submitted to the Graduate Faculty

in Partial Fulfilment of the Requirement

for the Degree of

Master of Science

in the Department of Companion Animals

Faculty of Veterinary Medicine

University of Prince Edward Island

Everardo M. Salinas-Navarrete

Charlottetown, P.E.I.

September, 1998

CONDITIONS OF USE

SIGNATURE PAGES

iii-iv

REMOVED

ABSTRACT

Pathological alterations and infiltration of T-lymphocytes into the renal cortex of dogs with naturally occurring renal diseases are important in the initiation and progression of renal failure in animals and human beings. Quantification of morphological alterations and identification of the subsets of T-lymphocytes which infiltrates into the canine renal interstitium have not been studied. The objectives of our study were to quantify the histopathological alterations and to characterize the subsets ($CD4^+$ and $CD8^+$) of infiltrating T-lymphocytes by using morphometrical and immunohistochemical techniques, respectively, in renal tissue from dogs with naturally occurring renal disease.

Pathologic alterations in the renal cortex were analyzed morphometrically from 39 dogs. Fields from the tissue sections were randomly selected and stereological methodology for morphometry was used. Eleven variables were measured. After morphometry, histopathological categorization was made and grouped (control (I), chronic interstitial nephritis (II), glomerulonephritis (III), amyloidosis (IV), nephrocalcinosis (V) and glomerulonephritis (VI)) according to histopathological findings and final diagnosis submitted by a pathologist from the Atlantic Veterinary College Diagnostic Laboratory. Kidney tissues from normal dogs were used as a control group. Data was analyzed with Minitab statistical software program. A multiple comparison showed that the interstitial and tubular volume fraction measurements differed significantly between the control group and groups II, III, IV and VI. Bowman's capsule harmonic thickness was significantly increased in group III. The absolute volume of interstitium showed a significant tendency to increase with increasing creatinine levels. There was a strong correlation between serum creatinine concentration and interstitial or tubular volume fraction. A prediction equation obtained from multiple regression analysis of serum creatinine concentration with interstitial volume fraction and glomerular area was statistically significant ($p<0.05$) (y=-433+1300(interstitial volume fraction)+0.00905(glomerular area), $r^2=0.48$). The equation was standardized (y=358+184(interstitial volume fraction)+122(glomerular area), $r^2=0.48$) to demonstrate which independent variable had a greater impact on serum creatinine concentration. The standardized equation demonstrates that interstitial volume fraction has a greater impact on serum creatinine concentration than glomerular area. In conclusion, the present study revealed that serum creatinine concentration (used as a measure of renal function) correlates more strongly with tubulointerstitial abnormalities than with glomerular abnormalities in dogs with natural occurring renal disease.

The subsets of T-lymphocytes were identified by applying monoclonal antibody to frozen renal tissue sections from 14 dogs. Fields from tissue sections were randomly selected. Positively stained $CD4^+$ and $CD8^+$ cells were enumerated. After cell identification, histopathological categorization was made and grouped (control (I), mild (II), moderate (III) and severe (IV)) according to the degree of glomerular and tubulointerstitial inflammatory cell infiltration and interstitial fibrosis. Mesenteric lymph node and kidney tissue from normal dogs were used as positive and negative controls. Data were analyzed with a Minitab statistical software program. Kidney tissue from normal dogs had no T-lymphocytic infiltration. Groups with a higher degree of glomerular and tubulointerstitial inflammatory

cell infiltration and interstitial fibrosis had a higher number of $CD4^+$ and $CD8^+$ T-lymphocytes. However, a multiple comparison on the total number of $CD4^+$ and $CD8^+$ T-lymphocytes between groups showed that control group and group IV were the only statistically different groups. In conclusion, the present study revealed that $CD4^+$ and $CD8^+$ T-lymphocytes are present within the renal interstitium of dogs with naturally occurring renal disease. The proportion of $CD4^+$ versus $CD8^+$ T-lymphocytes is similar in diseased kidneys. The number of $CD4^+$ and $CD8^+$ T-lymphocytes increase with the severity of histopathological renal lesions.

ACKNOWLEDGMENTS

I would like to thank the members of my supervisory committee, Drs. B. Hill, B. Horney, D. Shaw, L. Miller and W. Ireland. I particularly thank my supervisor, Dr. D. Shaw and also, Dr. W. Ireland, for their guidance and input into this research.

I am extremely grateful to Dr. A. Lopez for giving me the opportunity to come to the Atlantic Veterinary College and to be a part of the CIDA cooperation project between the University of Prince Edward Island and the Universidad Autonoma de Tamaulipas.

I would also like to thank the Canadian International Development Agency (CIDA) for its support of my tuition and student stipend.

I acknowledge and I am grateful for the financial support of the research by the Atlantic Veterinary College (AVC) research fund.

I would like to thank M.V.Z. Fernando Arizpe Garcia, from the Universidad Autónoma de Tamaulipas and M.V.Z. Sergio Garza Quiroga, Dean of the Faculty of Veterinary Medicine of the Universidad Autónoma de Tamaulipas.

I thank my wife, Carmen, and our daughter, Mariana. None of this would have been possible without their support.

I thank all my friends that I have made here in the AVC, particularly Jean Lavallée and Gabino Peñalver.

TABLE OF CONTENTS

LIST OF FIGURES

LIST OF TABLES

ABBREVIATIONS USED IN THE TEXT

Term	Abbreviation
A_A	area fraction
ABC	avidin-biotin complex
AVC	Atlantic Veterinary College
bwsA	Bowman's space area
BQ	Bioquant system
$capV_V$	capillary volume fraction
CRF	chronic renal failure
DAB	diaminobenzidine
GFR	glomerular filtration rate
glomA	glomerular area
$glomV_V$	glomerular volume fraction
harT	Bowman's capsule harmonic thickness
IHC	immunohistochemistry
$intV_V$	interstitial volume fraction
mm	millimeters
NA	not available
PAS	periodic acid schiff
PBS	phosphate buffered saline
PDGF	platelet-derived growth factor
r	correlation coefficient
R^2	squared multiple correlation coefficient
SD	standard deviation
TGF-β	transforming growth factor beta
tlV_V	tubular lumen volume fraction
$tubV_V$	tubular volume fraction
tuftA	glomerular tuft area
twV_V	tubular wall volume fraction
V_V	volume fraction
vwmvg	volume weighted mean volume of the glomerulus
%	percent
μmol/L	micro moles per liter
μm	micromiters
μm^2	squared micromiters
μm^3	cubic micromiters

GENERAL INTRODUCTION

Chronic renal failure (CRF) is the most common sequela of renal disease in dogs and cats (1). Chronic renal failure is an irreversible and progressive disease and is a common cause of death in dogs and cats of all ages. There is no curative treatment but the clinical and biochemical consequences of reduced renal function can be minimized by symptomatic and supportive therapy. The estimated population of dogs and cats in the Maritime provinces (Prince Edward Island, New Brunswick and Nova Scotia) is 398,375 cats and 355,844 dogs (Table I). The percentages of the dog and cat population examined by a veterinarian in the USA are 70% and 92% respectively (American Animal Hospital Association). The annual prevalence of CRF in cats and dogs examined by a veterinarian in the USA is 1.6% and 0.9%, respectively (1). Analyzing this information and assuming that: 1) pet ownership characteristics are similar in the Maritime provinces as compared to the USA; 2) pet owners utilize veterinary services with similar frequency in the Maritime provinces as compared to the USA; and 3) the prevalence of CRF in the dog and cat population in the Maritime provinces is similar to the USA; it is estimated that 4462 cats and 2947 dogs will develop CRF every year (Table II).

Table I. Number of Dogs and Cats in the Maritime Provinces

(From Dr. Darcy Shaw, Department of Companion Animals University of Prince Edward Island, Canada)

	Human population*	# Households*	% Households owning cats**	% Households owning dogs**	Ave. # cats/cat owning household**	Ave. # dogs/dog owning household**	Estimated population of cats	Estimated population of dogs
PEI	134,657	48,630	27.3	31.6	2.19	1.69	29,074	25,970
New Brunswick	738,133	272,915	27.3	31.6	2.19	1.69	163,168	145,748
Nova Scotia	909,282	344,779	27.3	31.6	2.19	1.69	206,133	184,126
Totals	1,782,072	666,324					398,375	355,844

*1996 Census, Population and Dwelling Counts, Statistics Canada

**Gehrke BC. Results of the AVMA survey of US pet-owning households on companion animal ownership. J Am Vet Med Assoc 1997; 211: 169-170.

Table II. Calculation* of the number of dogs and cats that will develop chronic renal failure (CRF) in the Maritime provinces

(From Dr. Darcy Shaw, Department of Companion Animals University of Prince Edward Island, Canada)

	Estimated pop. of cats	Estimated pop. of dogs	% of cats examined	% of dogs examined	Prevalence of CRF in cats examined (%)	Prevalence of CRF in dogs examined (%)	Estimated # of cats with CRF	Estimated # of dogs with CRF
PEI	29,074	25,970	70	92	1.6	0.9	326	215
New Brunswick	163,168	145,748	70	92	1.6	0.9	1827	1207
Nova Scotia	206,133	184,126	70	92	1.6	0.9	2309	1525
Totals	398,375	355,844					4462	2947

* Calculation on an annual basis

Estimated prevalence of CRF (1)

Cats = 1.6% of cats examined by a veterinarian

Dogs = 0.9% of dogs examined by a veterinarian

Percentage of the dog and cat population examined by a veterinarian (The 1995, AAHA report)

Cats = 70% of cats visit a veterinarian at least once a year

Dogs = 92% of dogs visit a veterinarian at least once a year

Chronic renal failure is associated with a number of morphologic changes in renal structure. Alterations in the glomerulus can include the deposition of preformed immune complexes (antigen-antibody) in the glomerular capillary wall, thickening of the basement membrane, mesangial cell proliferation, extracellular deposition of proteins, and infiltration of immune and inflammatory cells. Alterations in the tubulointerstitium can include mononuclear cell infiltration (e.g. macrophages, lymphocytes), tubular cell degeneration and atrophy, and interstitial fibrosis. These lesions occur in various renal disorders in animals and human beings (2,3).

Tubulointerstitial fibrosis with varying degrees of mononuclear inflammatory cell infiltration is the final common histopathologic pathway for the majority of kidney diseases that progress towards end-stage renal failure (4). The functional importance of tubulointerstitial fibrosis in human beings has been documented by many researchers (5-10). Tubulointerstitial fibrosis is characterized by the stimulation and proliferation of interstitial fibroblasts resulting in the production and deposition of large amounts of extracellular matrix (11).

Maintenance of the normal architecture and biological functions of the kidney depend on well integrated cellular and extracellular matrix structural interactions. Any alteration in the composition and structure of the extracellular matrix may have important consequences on the functional integrity of the nephron (11).

Morphometrical methods are used to quantify structural alterations in the glomerulus and tubulointerstitium (12) and permit correlation of these changes to biochemical indicators of renal function. Stereology (13), a subset of morphometry, can be used to measure the

volume fraction of glomeruli, tubules, peritubular capillaries, and interstitium, and to measure glomerular structures such as glomerular area, glomerular tuft area, Bowman's space area, Bowman's capsule thickness and volume weighted mean volume of glomeruli in the kidney. The application of stereological methods in the first part of this study allowed the correlation of the cited renal measurements with serum creatinine concentration which was used as a biochemical indicator of renal function.

The infiltration of lymphocytes and macrophages into glomeruli and the tubulointerstitium plays an important role in the pathogenesis and progression of renal damage (14). Chronic interstitial nephritis in human beings is characterized by the presence of mononuclear inflammatory infiltrates with the majority being T-lymphocytes (15). These cells may lead directly or indirectly to the induction of tubulointerstitial fibrosis. The subsets of infiltrating T-lymphocytes in the canine renal intersititium are unknown. The second part of this research characterized some of these infiltrates, specifically $CD4^+$ and $CD8^+$ T-lymphocytes in various naturally occurring renal diseases in dogs.

These studies will help to identify and assess the relative impact of glomerular and tubulointerstitial abnormalities on renal function in dogs.

1. LITERATURE REVIEW

1.1. Morphometry of renal structures

1.1.1. Introduction

The form and shape of renal structures can be evaluated by using morphometric analysis. Morphometric methods, including stereological methods, have been widely used to analyze renal structures in both animals and human beings (12,16).

Stereology is defined as "a body of mathematical methods relating three-dimensional parameters defining the structure to two-dimensional measurements obtainable on sections of the structure" (13). In simple words, stereology is the study of three dimensional properties of objects usually seen in two dimensional samples, such as tissue sections. The main advantage of stereology is that it provides a useful method for obtaining reliable quantitative data on 3 dimensional structure, even when one is restricted to the study of 2 dimensional sections. Stereologic methods are particularly useful in biological morphometry (13).

1.1.2. Morphology and morphometry of normal kidneys

Macroscopically, the canine kidney consists of three main segments: the cortex, medulla and renal pelvis. The functional unit of the kidney, the nephron, extends from the cortex to the medulla and empties into the pelvis. One kidney contains approximately 430,000 nephrons in dogs, 190,000 nephrons in cats (17), 31,500 in the rats (18), and about

800,000 to 1,200,000 in human beings (19). Microscopically, the essential components of the nephron are the glomerulus and Bowman's capsule, proximal tubule, loop of Henle, distal tubule, connecting segment, and collecting duct (20).

The normal cortex/medulla volume ratio is approximately 1:2 or 1:3 in domestic animals (21). Renal medulla can be subdivided into an outer and inner medulla. The cortex is mainly composed of nephrons, interstitial space and blood capillaries. The major components of the medulla are the loops of Henle, medullary collecting ducts, interstitium and small vascular structures. Branching of the renal blood vessels starts at the renal artery which enters at the hilus and divides into interlobar arteries. At the corticomedullary junction, arcuate arteries arise followed by nearly straight interlobular arteries, which enter the cortex and burgeon into short afferent arterioles ending in the glomeruli (22).

Renal morphometry has been largely studied in rats and human beings. To our knowledge, little has been done regarding renal morphometry in dogs.

1.1.2.1. The renal interstitium

Morphometric studies have shown that the mean percentage volume of interstitial tissue in the normal renal cortex is 12.8±5.1% in human beings (23), and 7 to 9 % in the rats (19). In rats, 3 of the 7 % represents interstitial cells, while the remaining 4 % represents the extracellular space. A gradual increase occurs in interstitial volume from outer to inner medulla. Interstitial volume comprises 10 to 20 % in the outer medulla and approximately 30 to 40 % at the papillary tip in both the rat and rabbit (19,24).

The cellular components of the tubulointerstitium include tubular epithelium,

interstitial cells type I (fibroblast-like cell) and type II (lymphocyte-like cell) in the cortex, and types I, II (similar to the cortex) and III (perivascular cell) in the medulla, in addition to interstitial fibroblasts, vascular endothelium, nerve cells, lymphatics, macrophages, and lymphocytes (19). Extracellular matrix makes up the remainder of the interstitial compartment and contains collagen types I, III and VI, glycoproteins such as mucin, and interstitial fluid (25).

1.1.3. Morphometry of abnormal kidneys and correlation with renal function

1.1.3.1. Morphometry in human tissue

Quantitative morphometrical analysis of kidney structures in renal biopsies taken from human beings with various renal diseases has been described (6,8,9,10,26,27). Correlation between glomerular and tubulointerstitial measurements (volume fraction) and renal function (evaluated by serum creatinine concentration, glomerular filtration rate, or other measures) has also been studied (8,9). Results from these studies indicate that pathologic tubulointerstitial alterations are more closely associated with changes in renal function (serum creatinine concentration), than are pathologic changes in glomeruli. A reduction in glomerular filtration rate, effective renal plasma flow and concentrating ability of the kidney has been closely related to abnormalities of the tubulointerstitium, regardless of the type of renal disease (8). Investigations have documented a positive and significant correlation between the relative interstitial volume fraction of the renal cortex and serum creatinine concentration at the time of biopsy (9). This relationship has been demonstrated in moderately severe mesangioproliferative glomerulonephritis (10), chronic sclerosing

interstitial nephritides (26), inflammatory and noninflammatory glomerular diseases (6), glomerular amyloidosis (27), and other renal diseases in human patients. Similar observations have been found in rodent models of renal disease. In contrast, morphometric analysis of renal biopsies taken from human patients with perimembranous glomerulonephritis (28) and membranoproliferative glomerulonephritis with different grades of glomerular involvement (29), did not reveal a significant relationship between the severity of glomerular lesions and the serum creatinine concentration.

A study of 48 cases of renal amyloidosis in human beings revealed that in glomerular amyloidosis, there is a significant positive correlation between the increase in serum creatinine concentration and interstitial volume fraction (30). This investigation also revealed that renal function was influenced by interstitial fibrosis but not by amyloid accumulation in the interstitium. Studies of human cases of interstitial nephritis and glomerulonephritis (5) demonstrated that a decrease in the total area of proximal tubules or of tubular epithelial cells correlated with an increase in interstitial breadth thickness, due to fibrosis, and an increase in serum creatinine concentration. Morphometric analysis of renal biopsies from 40 men and women with renal amyloidosis and glomerulonephritis (31) showed that a significant positive correlation exists between cortical interstitial volume fraction and serum creatinine concentration, regardless of the severity and the type of glomerular disease. In addition, the same study revealed that a significant negative correlation existed between interstitial capillary area and an increase in interstitial volume fraction. Furthermore, a significant correlation was present between increased cortical interstitial volume fraction and decreased tubular cell volume fraction.

Inflammatory and noninflammatory glomerular diseases, even when very severe, are not accompanied by a measurable reduction in glomerular filtration rate when the renal cortical interstitium and the tubules are essentially normal (6).

The concentrating ability of the kidney depends primarily on tubulointerstitial function and not on glomerular filtration surface area. For instance, as interstitial fibrosis and tubular atrophy increase, the maximum concentrating ability of the kidney decreases (6). The concentrating ability of the kidney is frequently impaired when there is fibrosis and interstitial inflammation (either alone or accompanying another disorder). Because fibrosis can result in marked thickening (widening) of the interstitium and disruption of vasculature, the supply of oxygen and nutrients to the tubules is reduced leading to tubular atrophy (32).

The filtration function of the glomerulus, for substances usually eliminated in the urine (e.g. urea, creatinine), is also negatively affected by tubulointerstitial changes such as interstitial fibrosis and tubular atrophy (6).

There are different theories on the mechanism by which interstitial fibrosis decreases glomerular filtration rate (GFR) and increase serum creatinine concentration. Glomerular filtration rate can be normal under pathological conditions only when the outflow from the glomerular capillaries into the intertubular capillaries is not restricted (27). One theory suggests that if obliteration of the intertubular capillaries occurs due to interstitial inflammation and fibrosis, postglomerular vascular resistance increases. This would lead to increased pressure and dilation of the glomerular tuft capillaries (31). Glomerular filtration rate would decrease and result in an increased serum creatinine concentration (27). In addition, tubular atrophy secondary to interstitial fibrosis could result in tubular dysfunction

and result in a reduction in sodium chloride reabsorption. An increase in tubular fluid sodium chloride concentration at the macula densa could decrease GFR due to tubuloglomerular feedback (5,31). Consequently, as tubular function deteriorates, glomerular filtration rate can be reduced and elevate serum creatinine concentration. Therefore, data obtained from human beings indicates that pathologic changes in the renal interstitium are a prime determinant of reduced renal function and that glomerular and tubular function may be directly or indirectly affected by interstitial pathology.

1.2. Immunohistochemical analysis of renal inflammatory cells

1.2.1. Introduction

Histochemistry is based on the use of tinctorial stains for the visualization of nucleic acids, carbohydrates, proteins, lipids, enzymes, and microorganisms (33). Immunohistochemistry (IHC) is an advanced technique of histochemistry generally used to detect cell and tissue proteins. The objective of IHC is to identify cell and tissue antigens by *in situ* antigen-antibody reactions made visible by reporter molecules such as fluorochromes, enzymes, and colloidal gold particles (33). Immunohistochemistry has been used for the diagnosis of many diseases associated with autoantibodies, tumors, immune complex deposition, and for the detection of microorganisms in tissue sections (34).

Different immunohistochemical staining methods can be used to localize antigens in tissue sections. The direct staining technique involves conjugating the primary antibody and staining in one step. The advantages of this technique are the limited number of reagents and the short staining time. However, since staining involves only one labeled antibody, little

signal amplification is achieved and therefore, direct methods are less commonly used. In the indirect method, specific unconjugated primary antibody binds to the antigen of interest. An enzyme-labeled secondary antibody directed against the primary antibody is then applied. Subsequent use of a substrate-chromogen solution concludes the reaction sequence and a colored reaction is detected with light microscopy (35).

Other immunoenzyme techniques have been designed to amplify the visible signal as avidin-biotin complex (ABC) technique. Antigens in tissue sections are detected by an unlabeled primary antibody followed by a secondary antibody labeled with biotin which binds to the primary antibody. The tissue is then exposed to a preformed complex of avidin-biotin-enzyme which binds with high affinity to the biotinylated secondary antibody. The biotin molecules are labeled with an enzyme, commonly peroxidase or alkaline phosphatase. An enzyme substrate (e.g. diaminobenzidine if peroxidase is used) is then applied to the tissue and a colored reaction product forms at sites of antibody-enzyme complex binding (34).

1.2.2. Identification of inflammatory cells in abnormal kidneys

1.2.2.1. Inflammatory cells in the kidneys of human beings with renal disease

Studies in human beings with glomerulonephritis have demonstrated that interstitial leukocyte infiltration (predominantly T-lymphocytes) shows a strong correlation with impaired renal function (36). Interstitial leukocyte infiltration is an important component of most forms of glomerulonephritis and it plays a major role in both the pathogenesis and the progression of immunemediated glomerulonephritis. Studies of human

glomerulonephritidies have confirmed that T cells and macrophages play a major role in the induction of renal injury (37). These same studies have also shown that infiltration of the interstitium by mononuclear inflammatory cells is associated with the evolution of interstitial changes.

Chronic interstitial nephritis is characterized by tubular atrophy and interstitial fibrosis and may be the result of primary or secondary interstitial nephritis (15). Both forms of interstitial nephritis are initially characterized by the presence of inflammatory infiltrates consisting primarily of $CD4^+$ and $CD8^+$ T-lymphocytes (15).

Infiltration of mononuclear cells occurs within the glomeruli and renal tubulointerstitium in glomerular injury (38). Moreover, it is evident that glomerular macrophage infiltration occurs in most forms of glomerulonephritis (14). However, macrophage accumulation within the tubulointerstitium also plays a major role in renal injury and may, in fact, represent an important pathway for progressive renal injury (14).

1.2.2.2. Inflammatory cells in the kidney of other species with renal disease

Immunohistochemical studies in rats have demonstrated that the interstitium of chronically ischemic kidneys had a diffuse infiltration of mononuclear cells composed of B lymphocytes, $CD4^+$ T helper (Th1 and Th2) lymphocytes, and macrophages but very few $CD8^+$ cytotoxic T-lymphocytes (39). Th1 lymphocyte-activated macrophages have an enhanced ability to kill infected cells. Th2 lymphocytes activate antigen-binding B lymphocytes to differentiate into antibody-forming plasma cells. $CD8^+$ cytotoxic T lymphocytes target and kill infected cells.

Rats with autoimmune tubulointerstitial nephritis induced by immunization with bovine tubular basement membrane antigens have mononuclear infiltrates in the interstitium. These infiltrates include polymorphonuclear leukocytes, T-lymphocytes, and monocytes/macrophages in affected kidneys (40). This study also showed that T-lymphocytes, particularly $CD4^+$, play an important role in the development, progression, and regulation of tubulointerstitial nephritis. Specific cytokines released by $CD4^+$ T cells bind to proximal tubular epithelium and transcriptionally down-regulate the expression of type IV collagen (41).

In rats with proteinuria and tubulointerstitial nephritis induced by protein-overload, a significant increase in the number of T-lymphocytes was observed. The same study showed a strong positive correlation between the severity of tubulointerstitial nephritis and the degree of proteinuria. This suggests that proteinuria may play a direct role in the pathogenesis of tubulointerstitial injury which develops in association with chronic glomerulonephritis (42).

Three stages of progressive fibrogenesis are recognized as a sequella of inflammation (43). Stage 1 involves the events initiating and establishing the conditions essential for the promotion of active remodeling of the extracellular matrix which is mediated by cytokines, growth factors like transforming growth factor-β, interleukin-1, platelet derived growth factor and transforming growth factor-α. Active deposition of fibrotic matrix, and its disruptive effects on organ function are characteristic of stage 2. Stage 3 is the attenuation of the active deposition of fibrotic matrix. There are several tubulointerstitial cell types which may act as a target for inflammatory mediators, and whose activation is directly

responsible for synthesis of extracellular matrix. Among these are tubular epithelial cells, interstitial fibroblasts, and vascular endothelium (43).

1.3. Renal function (serum creatinine concentration)

The initial step in the excretory function of the kidney (nephron) is plasma filtration across the glomerulus. Filtrate enters Bowman's space, passes through the tubules and is modified by reabsorption and secretion. In general, the proximal tubule and loop of Henle reabsorb the bulk of the filtered solutes and water, while the collecting tubules make final small changes in urinary composition. The transtubular reabsorption or secretion of ions is facilitated by ion-specific channels (44).

Serum creatinine concentration can be used to evaluate renal function. Creatinine is produced from the metabolism of creatine in muscle. It is released into the blood at a relatively constant rate and is excreted largely by glomerular filtration (45). Creatinine is not significantly secreted or reabsorbed by the tubules (46). For this reason, serum creatinine concentration can be used to evaluate renal (glomerular) function. Increased serum creatinine is indicative of decreased glomerular filtration in dogs. However, in addition to renal disease, serum creatinine may be elevated due to prerenal factors such as dehydration or hypovolemia, or postrenal factors such as urethral obstruction or rupture of the urinary tract.

1.4. Study objectives

The present project was divided in two sections:

The first section was conducted to quantitatively evaluate histopathological changes in canine renal tissue from dogs with naturally occurring renal disease. The objectives were:

1. To quantify the histopathological alterations in renal tissue from dogs with naturally occurring renal disease.

2. To evaluate the association of glomerular and tubulointerstitial pathologic changes with serum creatinine concentration.

The second section was conducted to identify the subsets of infiltrating mononuclear cells in the canine renal interstitium. The objective was:

1. To characterize the subsets and observe the proportions of infiltrating $CD4^+$ and $CD8^+$ T-lymphocytes in renal interstitium of dogs with naturally occurring renal disease.

2. CORRELATION OF GLOMERULAR AND TUBULOINTERSTITIAL PATHOLOGIC CHANGES TO SERUM CREATININE CONCENTRATION

2.1. Introduction

The normal architecture of renal structures such as the glomerulus and tubulointerstitium is altered in a variety of kidney diseases (e.g. chronic interstitial nephritis, glomerulonephritis, amyloidosis, and others). Measurement of renal structures can give a numerical estimate of the severity of histopathological changes which then can be related to kidney function.

Creatinine, formed in muscle from degradation of creatine, is released in to the plasma at a relatively constant rate. Serum creatinine concentration is very stable and tends vary inversely with the glomerular filtration rate in the steady state (46). Because of this relationship, measurement of the serum creatinine concentration can be used to assess renal function (glomerular filtration rate).

Quantitative morphological changes in the kidney of dogs with and without naturally occurring renal disease were evaluated using stereological methodology.

An association between pathologic changes in the glomerulus and tubulointerstitium with serum creatinine concentration, was investigated in a preliminary and a main study.

2.2. Pilot study

A pilot study was performed to standardize the tissue section thickness, the number of sections/tissue block (cuts at different depth levels), tissue staining technique, and the methods of morphometric analysis.

2.2.1. Materials and methods

2.2.1.1. Selection of cases

Thirty-four canine renal tissue specimens with histopathological changes (disease groups) and five canine renal tissue specimens without histopathological abnormalities (control group), were selected retrospectively. Each specimen came from dogs that had a recent measurement of serum creatinine concentration close to time of death or euthanasia. The specimens were selected from the Atlantic Veterinary College (AVC) Diagnostic Laboratory database. Every specimen which met the selection criteria (i.e., sufficient preserved renal tissue, recent serum creatinine measurement), was used in the study. A total of 34 cases were identified between 1988-1997 and all of these cases were analyzed without any further addition or deletion of cases.

Blocks of kidney tissue from 10 of the selected cases (one used as a control) were obtained and used for a pilot morphometric analysis. Selection was made to obtain a range of serum creatinine concentration from normal to markedly abnormal (54-1205 μmol/L). The remaining 29 cases were evaluated in the main morphometric analysis.

2.2.1.2. Slide preparation and staining (preliminary study)

From each renal tissue block, two five micron thick sections were cut at three different depth levels two-hundred microns apart (six sections per block). The depth levels were chosen to avoid sampling the same renal cortex structure (e.g., glomerulus) twice. Tissue sections from each depth level were stained with either periodic acid schiff (PAS) with a hematoxylin counterstain (three sections) or Masson's trichrome (three sections). The two stains were used to determine which was superior for renal structure identification.

2.2.1.3. Random selection of fields from outer, middle and inner cortex

Using light microscopy at a magnification of 6.3 X, the cortex was divided from the medulla on each slide. The corticomedullary junction was demarcated with a line on the slide.

Random selection of one field from each part of the cortex (outer, middle and inner) was made using a 26 × 76 mm plastic grid (same size as the microscope slide) with 533 points. The grid was placed under each slide (Figure 1). The number of points which contacted each part of the cortex were counted and multiplied by random number chosen from a random number table. The resulting value was the random field number and this was demarcated with a marker. A total of 9 fields were selected from each case, one from the outer, middle and inner cortex of each of the three sections obtained at different depths.

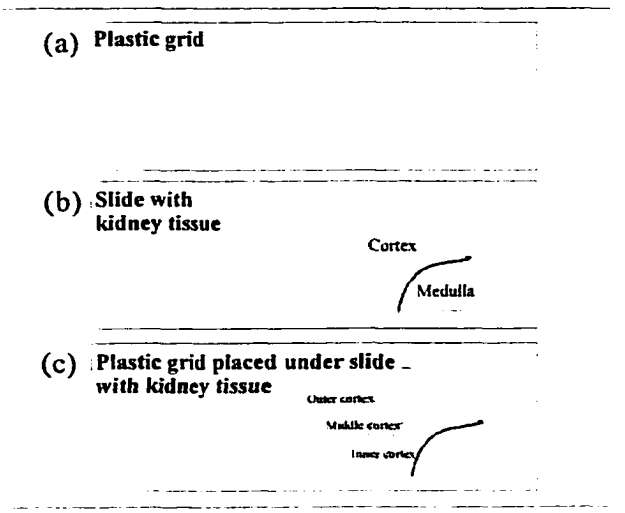

Figure 1. Random selection of fields from renal cortex. Plastic grid (a) is placed under salide with kidney tissue (b). The points that hit each part of the cortex (c) are counted and multiplied by random number chosen from a random number table.

2.2.1.4. Morphometry

Morphometry was performed without knowledge of the histopathological diagnosis. Furthermore, slides from different cases were mixed together before quantification.

Morphometrical principles

Four main morphometrical parameters were considered in this part of the study: volume fraction (e.g., renal interstitial volume fraction per volume of cortex), relative area (e.g., glomerular area, glomerular tuft area and Bowman's space area), barrier harmonic mean thickness (e.g., Bowman's capsule harmonic thickness), and volume weighted mean volume of glomeruli in the kidney. Relative volume fraction (V_V) is the ratio of the volume of the structure of interest (e.g. renal interstitium, renal tubules, glomeruli) to the volume of the reference compartment (e.g. renal cortex) (12). For estimation of the volume fraction

variables, the entire field (i.e., renal cortex) was always used as the reference compartment. Glomerular, glomerular capillary tuft, and Bowman's space projected area were determined from glomeruli found in each random field. Barrier thickness refers to the thickness of a layer of tissue (e.g. Bowman's capsule) separating two spaces (e.g. Bowman's space from tubulointerstitial space). Bowman's capsule harmonic thickness was obtained from the same glomeruli used to determine surface areas. Volume weighted mean volume refers to the mean particle volume obtained from the volume distribution of the particle volumes (12), meaning that the estimates are weighted by larger particles. Volume weighted mean volume of the glomeruli was obtained from measurements performed on an average of 135.8 randomly selected glomeruli/case with a range from 60 to 155 glomeruli/case.

For volume fraction estimation (V_V) there are three options: 1) estimate directly the relative area occupied by profiles; 2) linear integration; and 3) point counting (47). Point counting with a systematic lattice grid was used in this study. This method was chosen because it is the most efficient (47).

The Bioquant system® (R&M Biometrics, Inc. Nashville, TN) (BQ) was used to estimate glomerular projected area (glomA), glomerular projected tuft area (tuftA), Bowman's capsule harmonic mean thickness (harT), and the volume weighted mean volume of glomeruli (vwmvg).

All measurements were recorded in a QuattroPro® (1996, Corel corporation limited. Ontario, CA) spreadsheet.

2.2.1.4.1. Point counting method

The point counting method was used to estimate the volume fractions: interstitial volume fraction ($intV_V$), tubular wall volume fraction (twV_V), tubular lumen volume fraction (tlV_V), capillary (peritubular) volume fraction ($capV_V$) and glomerular volume fraction ($glomV_V$). Tubular volume fraction ($tubV_V$) was obtained by the addition of tubular wall and tubular lumen volume fraction ($twV_V + tlV_V$).

When using point count with a test grid, the number of points overlying each structure of interest (P) divided by the number of points overlying the reference space ($_P$) is directly proportional to area fraction (A_A) and hence volume fraction (V_V)(equation 1)(12).

Equation 1

$$(P_P = A_A = V_V)$$

Volume fraction measurements

Using 250 diameters magnification (25X) at the light microscopic level, each marked random field was brought in focus and the field mark was erased. A one-hundred square lattice grid was placed in the right ocular lens, but only twenty-five points as defined by the intersection between grid lines were used (Figure 2). One field with an area of 90,000 μ^2 was analyzed from the outer, middle and inner cortex for each of the three sections obtained at different depth levels. A total of 9 fields were analyzed from each case. Utilizing equation 1, the number of points hitting the structure of interest/25 points from reference space was

an estimate of the volume fraction of that structure. Values obtained from the nine fields for each parameter were averaged to estimated the volume fraction of the parameter or structure of interest for each case.

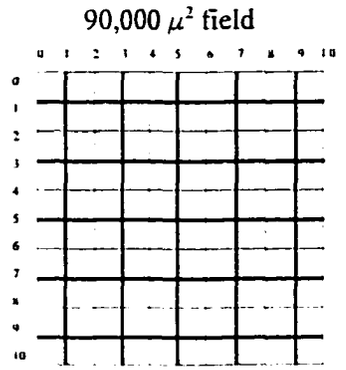

Figure 2. A one-hundred square lattice grid as seen through the ocular lens. Only points (25) defined by the intersection between darker lines were used.

2.2.1.4.2. Bioquant system

The Bioquant system (BQ) is composed of a digitizing pad as well as computer hard and software (Figure 3). The BQ software is supplemented with television camera (JE3012/A, Javelin Electronics), which receives information from a light microscope (Carl Zeiss, Canada Ltd., Don Mills, ON) and then is projected onto a computer monitor screen. The information from the digitizing pad (Hipad Digitizer Model: Dt1 1, Houston Instruments, Austin, Tx.) interfaced to the computer can measure the area of the image projected onto the

monitor and the areas of interest (e.g. glomerulus) from the tissue section were measured. Micrometers (μm) were the unit of measurement for glomerular area (μm^2), Bowman's capsule harmonic mean thickness (μm) and volume weighted mean volume of the glomerulus (μm^3). Calibration of the image magnification on the monitor screen was performed using a stage objective micrometer.

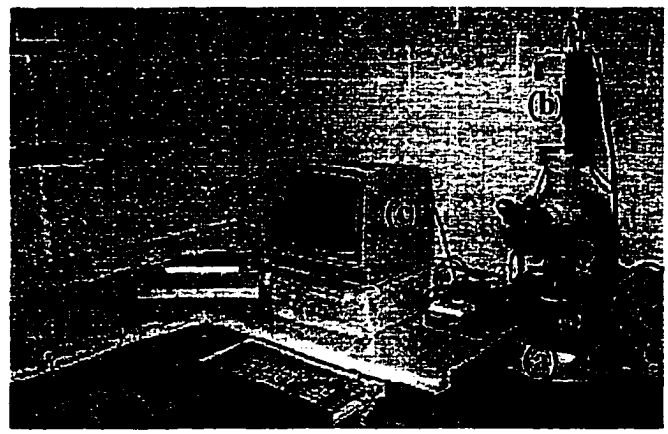

Figure 3. Bioquant system: light microscope (a), television camera (b), computer monitor screen (c), digitizing pad (d).

Glomerular measurements

Glomerular area

From a glomerulus found in each random field, glomerular projected area was measured with the BQ system (Figure 4). If a glomerulus was not found in a random field, the nearest glomerulus to the field was brought to focus and measured. A magnification of 63 diameters (6.3 X) or 160 diameters (16 X) at the light microscope level was chosen

depending on the size of each glomerulus. Final magnifications of the image on the monitor screen were 404X or 1018X, respectively. This was obtained by calibration using a stage micrometer. Bowman's space area was obtained by subtracting glomerular tuft area from glomerular area.

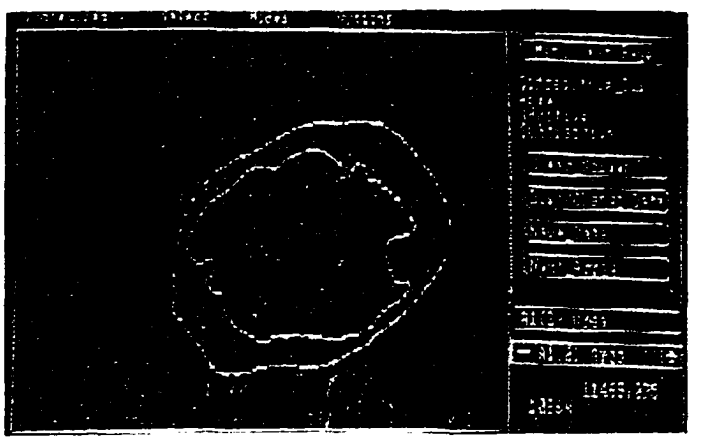

Figure 4. Glomerular area and glomerular tuft area measured with the Bioquant system.

Bowman's capsule harmonic thickness

Bowman's capsule harmonic mean thickness was estimated by placing a multipurpose Merz grid on the monitor screen and where grid lines intersected Bowman's capsule in random directions, the thickness was measured (Figure 5). Using this procedure, both the arithmetic mean and harmonic mean thickness can be estimated. Harmonic mean

thickness is a more stable and efficient estimator (12). Bowman's capsule harmonic mean thickness was estimated according to the following procedure (equation 2)(48):

a) Identify randomly directed lines (Merz grid) which cross Bowman's capsule

b) Measure the length (Li) of each line which contacts Bowman's capsule

c) Calculate the reciprocal of each length (1/Li)

d) Calculate the mean of the reciprocals (Σ1/Li)/n

e) Calculate the reciprocal of the mean of the reciprocals (d)

f) Multiply the reciprocal of the mean by 2/3

Equation 2

$$Th = (1/\frac{\Sigma 1/Li}{n}) \times \frac{2}{3}$$

where Li is the measured length, n is the number of measurements, and Th is harmonic mean thickness.

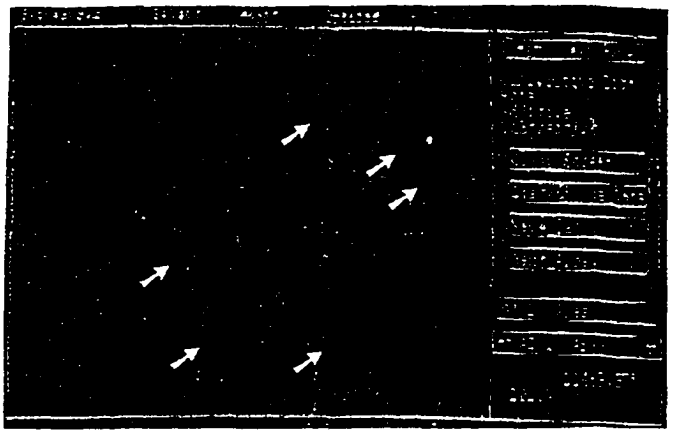

Figure 5. Glomerulus projected onto the computer screen monitor. Grid lines intersecting Bowman's capsule (white arrows) were measured.

Volume weighted mean volume of the glomeruli

Volume weighted mean volume of the glomeruli was measured at 63 diameters magnification (6.3 X). Final magnification of the image on the monitor screen was 404 X. The entire renal cortex on each slide was searched for glomeruli contacting points of the Merz grid. Approximately one hundred and forty intercept measures through those points that hit glomeruli were used to estimate volume weighted mean volume (Figure 6). The direction of the intercepts must be isotropic, uniform, and random with respect to the particle (glomerulus). Isotropic means that all directions in three dimensional space are equally likely, while uniform implies that all positions in the three dimensional space are equally likely (12). Between 150 to 200 measurements are needed to obtain a reliable estimate of volume weighted mean volume of glomeruli. Point sample intercepts provide unbiased estimates of the volume weighted mean volume (V_v) of arbitrary particles (e.g., glomeruli) (49).

The volume weighted mean volume of the glomerulus was calculated using the following procedure (equation 3)(12): when a point from the Merz grid contacted a glomerulus, a random direction through that point was chosen, the intercept length through that point was measured, and then the value was used in equation 3.

Equation 3

$$\overline{Vv}=(\pi/3)\times(\Sigma l^3/n)$$

where $\pi/3$ is a constant, Σl^3 is the average of the cubed intercept lengths, and V_v is the volume weighted mean volume of glomeruli for that case (12).

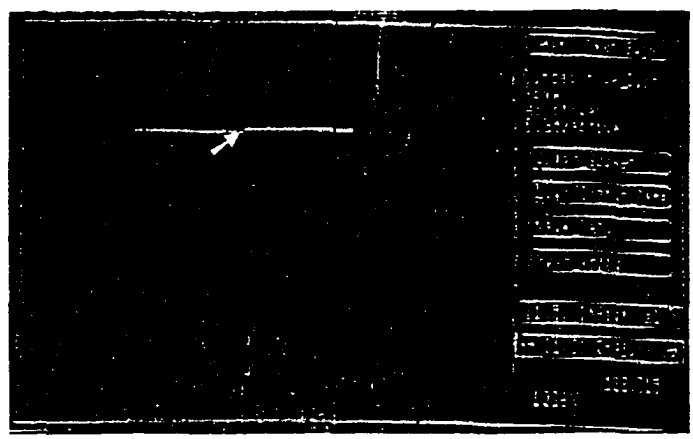

Figure 6. Photograph of glomerulus hitting points of Merz grid. Intercept (white arrow) length measured (white line).

2.2.1.5. Statistical analysis

Using the Minitab® (1994, Minitab Inc. State college PA) statistical software program, one way analysis of variance was used to test for significant differences between sections at the three different depth levels (200μ apart), and within fields from different levels of the cortex (i.e., outer, middle and inner). A P value of <0.05 was considered significant.

Pearson correlation was performed to detect any association of serum creatinine concentration to the measured variables.

2.2.2. Results

After slides stained with either PAS/hematoxylin counterstain or Masson's trichrome were examined, PAS/hematoxylin counterstain was judged to provide superior structure definition.

A total of ninety fields was examined from the 10 histological specimens. Eleven variables were measured to standardize the morphometric analysis: interstitial volume fraction(intV_V), tubular wall volume fraction (twV_V), tubular lumen volume fraction (tlV_V), tubular volume fraction (tubV_V) capillary volume fraction (capV_V), glomerular volume fraction (gV_V), glomerular area (glomA), glomerular tuft area (tuftA), Bowman's space area (bwsA), Bowman's capsule harmonic thickness (harT) and volume weighted mean volume of glomeruli (vwmvg). For each variable, the average number from the nine fields was reported (Table III).

No statistically significant difference ($p>0.05$) was found between the measurements

made from the tissue sections obtained at different depth levels.

No significant difference ($p>0.05$) was observed between the measurements taken from the random fields in outer, middle and inner cortex.

The correlation coefficient between serum creatinine concentration and the measured variables were as follows (Table IV): interstitium volume fraction (r^2=51.8%, r=0.72, p=0.01), tubular volume fraction (r^2=27%, r=-0.52, p=0.12), capillary volume fraction (r^2=10.8%, r=0.33, p=0.33), glomerular volume fraction (r^2=0.16%, r=0.04, p=0.90), glomerular area (r^2=30%, r=0.55, p=0.10), glomerular tuft area (r^2=7.2%, r=0.27, p=0.43), Bowman's space area (r^2=37%, r=0.61, p=0.05), Bowman's harmonic mean thickness (r^2=12.9%, r=0.36, p=0.30), volume weighted mean volume of the glomerulus (r^2=3.2%, r=0.18, p=0.60).

Table III. Quantification of renal structures (preliminary study)

Case No.	Serum creat. µmol/L	Volume fraction(%) variables* (mean ± 1 SD)						Glomerular variables** (mean ± 1 SD)				
		$intV_V$	twV_V	tlV_V	$tubV_V$	$capV_V$	$glomV_V$	glomA μm^2	tuftA μm^2	bwsA μm^2	harT µm	vwmvg μm^3
1	54	0.4178 ±0.1022	0.3467 ±0.0800	0.1511 ±0.0558	0.4978 ±0.077	0.0010 ±0.00	0.088 ±0.0819	10032 ±3174	5633 ±2368	4398 ±1851	2.051 ±0.660	1148079
2	68	0.3156 ±0.1542	0.3467 ±0.0917	0.2356 ±0.1174	0.5822 ±0.1576	0.0010 ±0.00	0.1022 ±0.1022	34964 ±9340	15752 ±7252	19212 ±5085	2.490 ±0.812	631094
3	87	0.3467 ±0.1183	0.3067 ±0.1311	0.2400 ±0.0566	0.5467 ±0.1386	0.0010 ±0.00	0.1067 ±0.1637	29212 ±11056	15153 ±6141	14059 ±6383	3.738 ±1.847	7639570
4	110	0.4533 ±0.0917	0.2489 ±0.0558	0.2222 ±0.0777	0.4711 ±0.0657	0.0010 ±0.00	0.0711 ±0.0955	15566 ±2540	7985 ±1943	7581 ±1995	1.937 ±2.066	2305921
5	281	0.3556 ±0.0811	0.2133 ±0.0566	0.1467 ±0.0748	0.3600 ±0.0917	0.0054 ±0.0133	0.2578 ±0.1601	26314 ±8250	11533 ±3392	14781 ±5648	6.10 ±3.29	4027473
6	351	0.4089 ±0.1015	0.1644 ±0.0882	0.2400 ±0.0980	0.4044 ±0.1503	0.0054 ±0.0133	0.1689 ±0.2067	31832 ±7501	12010 ±8592	18822 ±12046	2.632 ±0.923	4775466
7	691	0.4044 ±0.1157	0.2400 ±0.1095	0.2800 ±0.1058	0.5200 ±0.1296	0.0098 ±0.0176	0.0756 ±0.0786	29438 ±8945	10967 ±7149	18611 ±6995	3.219 ±1.544	5145520
8	779	0.4311 ±0.1229	0.1689 ±0.0558	0.1289 ±0.0843	0.2978 ±0.1097	0.0810 ±0.0600	0.1778 ±0.0961	19475 ±3310	8640 ±2301	10834 ±3585	7.352 ±1.510	3178950
9	1036	0.4533 ±0.1296	0.1956 ±0.0989	0.3111 ±0.1229	0.5067 ±0.1265	0.0010 ±0.00	0.0444 ±0.0968	33786 ±15108	6990 ±4071	26795 ±17212	4.516 ±1.517	4462315
10	1205	0.5511 ±0.1261	0.1022 ±0.0667	0.1956 ±0.0786	0.2978 ±0.100	0.0098 ±0.0176	0.1378 ±0.200	44303 ±11992	23240 ±9675	21063 ±8376	3.098 ±0.714	6403348

* $intV_V$ = interstitial volume fraction, twV_V = tubular wall volume fraction, tlV_V = tubular lumen volume fraction, $tubV_V$ = tubular volume fraction, $capV_V$ = capillary volume fraction, $glomV_V$ = glomerular volume fraction.

** glomA = glomerular area, tuftA = glomerular capillary tuft area, bwsA = Bowman's space area, harT = Bowman's capsule harmonic mean thickness, vwmvg = volume weighted mean volume of the glomeruli.

Table IV. Association between serum creatinine concentration and measured cortico-renal variables.
(preliminary study n=10)

Variables analyzed	Serum creatinine concentration		
	Correlation coefficient		P values
Interstitial volume fraction	r^2=51.8%*	r=0.72*	P=0.01
Tubular volume fraction	r^2=27%	r=0.52	P=0.12
Capillary volume fraction	r^2=10.8%	r=0.33	P=0.33
Glomerular volume fraction	r^2=.16%	r=0.04	P=0.90
Glomerular area	r^2=30.2%	r=0.55	P=0.10
Glomerular tuft area	r^2=7.2%	r=0.27	P=0.43
Bowman's space area	r^2=37.2%*	r=0.61*	P=0.05
Bowman's capsule harmonic mean thickness	r^2=12.9%	r=0.36	P=0.30
Volume weighted mean volume of glomerulus	r^2=3.2%	r=0.18	P=0.60

*statistically significant correlation coefficient

2.2.3. Discussion

Acceptable visual definition of renal structure (glomeruli, tubules, Bowman's capsule, interstitium) is required to perform morphometrical analysis. Periodic acid schiff with hematoxylin counterstain was judged to provide superior structure definition.

In view of the fact that there was no statistical difference between measurements taken at different depth levels, only one slide per block of kidney tissue was considered necessary for quantitative analysis on the remaining cases (main study).

Although there was no significant difference between outer, middle, and inner cortical measurements, because only one slide was made for the main study, three randomly selected fields from each part of the cortex were taken to ensure acceptable sample size. Therefore, nine fields per slide were analyzed in the main study instead of three fields per slide as were used in the preliminary study.

Of all variables measured, only interstitial volume fraction and Bowman's space area had a statistically significant correlation with serum creatinine concentration. The strength of association between serum creatinine and the measured variables may change when more data are analyzed in the main study.

2.2.4. Conclusion (pilot study)

Due to superior anatomical structure definition, only PAS with hematoxylin was used as the stain for the main study.

Only one (5μ thick) tissue section per block of kidney tissue would be required for the main study.

Nine randomly selected fields, three from the outer, middle, and inner cortex, were examined on each slide for the main study.

2.3. Main study

2.3.1. Materials and methods

2.3.1.1. Slide preparation and staining

From the remaining 29 blocks of kidney tissue (four used as a controls) single five micron thick sections were cut from each block. Sections were stained with PAS with a hematoxylin counterstain (50).

2.3.1.2. Random selection of fields from outer, middle and inner cortex

Corticomedullary junction was demarcated applying the same technique cited for the preliminary study in section 2.2.1.3.

Random selection of three fields from each part of the cortex (outer, middle and inner) was made according to methodology cited for preliminary study in section 2.2.1.3.1. A total of 9 fields (90,000 μ^2 /field) from each case were selected. A total area of 810,000 μ^2 was examined in each case.

2.3.1.3. Morphometry

Without knowledge of the histopathological diagnosis, the same quantitative techniques applied to tissue sections from the preliminary study were used in the main study (section 2.2.1.4.). Additional measurements such as the volume of kidney per nephron and

the absolute volume of interstitium and tubules per nephron were calculated by using the data obtained from the measurements of volume weighted mean volume of the glomerulus and the interstitial, tubular and glomerular volume fractions. Volume weighted mean volume of the glomerulus divided by glomerular volume fraction equals the volume of kidney per nephron. Volume of kidney per nephron multiplied by interstitial or tubular volume fraction equals to the absolute volume of interstitium or tubule per nephron.

2.3.1.4. Histopathological categorization groups

Selection was made according to the histopathological findings and final diagnosis submitted by pathologists from the Atlantic Veterinary College Diagnostic laboratory.

2.3.1.5. Statistical analysis

Cases from both the preliminary and main study were grouped for statistical analysis.

Descriptive statistics were performed on all the measurements per disease group on each variable. One way analysis of variance was performed (Minitab) to test for significant differences ($p \leq 0.05$) of each of the measured variables between disease groups.

For multiple comparisons Dunnett's analysis of variance was applied to test for statistically significant differences between the control group and disease groups.

Analysis of covariance was applied to compare the effects of groups adjusted to a common mean serum creatinine concentration (i.e., as though the 6 groups had the same mean serum creatinine concentration).

Pearson correlation was performed to detect any association of serum creatinine

concentration to the measured variables.

Multiple regression was performed to obtain an equation that uses one variable (dependent) to help explain the variation in another variable (independent). A P value equal to or less than 0.05 was considered significant.

2.3.2. Results

Six histopathological groups were identified from the 39 cases (Tables V-X): control group (5 cases), chronic interstitial nephritis group (18 cases), glomerulonephritis (11 cases), amyloidosis (3 cases), nephrocalcinosis (1 case) and granulomatous nephritis (1 case).

For each variable, results of the descriptive statistics are expressed as the mean ± 1 standard deviation for group (Tables XI-XII). To estimate volume weighted mean volume of the glomeruli, due to small tissue samples in some cases, the number of glomeruli measured per case ranged from 60 to 155 with an average of 135.8. Estimating about 135 instead of 150 to 200 measurements will only increase the standard deviation.

One way analysis of variance revealed that capillary volume fraction ($capV_V$, P=0.818), glomerular volume fraction ($glomV_V$, P=0.523), glomerular area (glomA P=0.436), glomerular tuft area (tuftA, P=0.787), Bowman's space area (bwsA, P=0.368) and volume weighted mean volume of the glomerulus (vwmvg, P=0.436) were not statistically different between histopathological groups. Interstitial volume fraction ($intV_V$, P=0.0002), tubular volume fraction ($tubV_V$, P=0.002) and Bowman's capsule harmonic mean thickness (harT, P=0.004) differed significantly between histopathological groups.

Multiple comparisons Dunnett's test showed that the interstitial and tubular volume

fraction measurements between the control group and groups two (chronic interstitial nephritis), three (glomerulonephritis), four (amyloidosis), and six (granulomatous nephritis) were statistically different (Figures 7,8). As interstitial volume fraction increases, tubular volume fraction decreases significantly as compared to normal values (control). Bowman's capsule harmonic mean thickness was significantly increased only in the glomerulonephritis group (Figure 9).

Analysis of covariance showed that the interstitial volume fraction increased significantly ($P<0.05$) as creatinine levels increased when data from all animals was analyzed and this was also true within disease groups. Tubular volume fraction decreased significantly ($P<0.05$) with increased serum creatinine concentration when data from all animals was analyzed and this was also true within disease groups. The absolute volume of interstitium/nephron (mm^3) showed a significant ($P<0.05$) tendency to enlarge with increasing serum creatinine concentration. This was not differentially ($P>0.05$) affected by disease group. The absolute volume of tubules/nephron (mm^3) was not significantly ($P>0.05$) affected with different serum creatinine concentration or with different disease group. Capillary volume fraction was not significantly ($P>0.05$) affected by either serum creatinine concentration or disease group. Glomerular volume fraction did not change significantly ($P>0.05$) with either serum creatinine concentration or disease group. Glomerular area showed a significant tendency to increase with increasing serum creatinine concentration. This increase was not due to an increase in glomerular capillary tuft area ($P>0.05$) but rather to a significant increase ($P<0.05$) in Bowman's space area and Bowman's capsule harmonic mean thickness. Volume weighted mean volume of the glomeruli were

not significantly (P>0.05) changed by either serum creatinine concentration or disease group.

The correlation coefficient (r) between serum creatinine concentration and the measured variables (data from all 39 animals) (Table XIII) were: interstitium volume fraction (r=0.58, p=0.00), tubular volume fraction (r=-0.56, p=0.00), capillary volume fraction (r=0.19, p=0.23), glomerular volume fraction (r=0.06, p=0.68), glomerular area (r=0.40, p=0.01), glomerular tuft area (r=-0.04, p=0.77), Bowman's space area (r=0.51, p=0.01), Bowman's harmonic thickness (r=0.45, p=0.004), volume weighted mean volume of the glomerulus (r=0.33, p=0.04). Correlation line graphs from these associations are presented in figures 10 to 18.

Three variable multiple regression (equation 4) was obtained between serum creatinine concentration as a dependent variable with interstitial volume fraction and glomerular area as a independent variables:

Equation 4

$$Cr = -433 + 1300 intVv + 0.00905 glomA \quad (R\text{-}sq = 48.2\%)$$

were Cr= serum creatinine concentration (μmol/L), $intV_V$= interstitial volume fraction (%), and glomA= glomerular area (μ^2). The equation was standardized:

$$Cr = 358 + 184 intVv + 122 glomA \quad (R\text{-}sq = 48.2\%)$$

by observing the value of the number in front of the variable (i.e., $intV_V$), it can be seen that interstitial volume fraction has about 1.5 times (184/122) the influence on serum creatinine than glomerular area.

Table V. Control group (5 cases)

Case No.	Signalment	Serum creatinine concentration (µmol/L)	Postmortem pathological diagnosis	Lab. No.
1	Female-spayed, Pug, 15 months.	99	Meningoencephalitis	c-21823
2	Female, Labrador retriever, 4 years.	70	Lymphomatoid granulomatosis	c-19341
3	Female-spayed, West Highland white terrier, 10 years.	60	Gastro-duodenal lymphosarcoma	c-878
4	Male, Mixed breed, 5 years.	71	Muscle atrophy	c-1983
5	Female-spayed, Brittany Spaniel. 10 years.	90	Generalized demodectic mange	c-16477

Table VI. Chronic interstitial nephritis group (18 cases)

Case No.	Signalment	Serum creatinine concentration (µmol/L)	Postmortem pathological diagnosis	Lab. No.
1	Female-spayed, Pembroke Welsh Corgi, 12 years.	162	Chronic Interstitial Nephritis	c-10998
2	Male, Daschund, 3.5 years.	651	Chronic interstitial nephritis	c-160
3	Female-spayed, Springer Spaniel, 3 years.	698	Chronic interstitial nephritis	c-4764
4	Male, Greyhound, 14 years.	691	Chronic interstitial nephritis	c-16416
5	Female-spayed, Springer Spaniel, 12 years.	219	Chronic interstitial nephritis	c-963
6	Female-spayed, Mixed breed, 8 years.	181	Chronic interstitial nephritis	c-2422
7	Female, Shetland Sheepdog, 5 years.	424	Chronic interstitial nephritis	c-701
8	Female, Collie blue, 9 years.	109	Chronic interstitial nephritis	c-14314
9	Male-neutered, Mixed breed, 3 years.	657	Chronic interstitial nephritis	c-12977
10	Female-spayed, Shepherd x, 14 years.	68	Chronic interstitial nephritis	c-4962
11	Female-spayed, Poodle, 11 years.	81	Chronic interstitial nephritis	c-5358
12	Male, Pug, 9 years.	52	Chronic interstitial nephritis	c-11655
13	Female-spayed, Mixed breed, 11 years.	79	Chronic interstitial nephritis	c-14
14	Female-spayed, German Shepherd, 8 years.	81	Chronic interstitial nephritis	c-12937
15	Female-spayed, Doberman pincher, 12 years.	90	Chronic interstitial nephritis	c-9853
16	Female, St. Bernard, 7 years.	109	Chronic interstitial nephritis	c-24591
17	Female-spayed, Kuvasz, 11 years.	601	Chronic interstitial nephritis	c-16623
18	Female, Shih tzu, 1 year.	976	Chronic interstitial nephritis	c-2516

Table VII. Glomerulonephritis group (11 cases)

Case No.	Signalment	Serum creatinine concentration (μmol/L)	Postmortem pathological diagnosis	Lab. No.
1	Female, Wheaton Terrier, 7 years.	181	Glomerulonephritis	c-20196
2	Female-spayed, Borzoi, 7 years.	281	Glomerulonephritis	c-21047
3	Female, Dalmation, 4 years.	621	Glomerulonephritis	c-11956
4	Male, Mixed, 8 years.	87	Glomerulonephritis	c-24063
5	Female-spayed, German Shepherd, 15 years.	102	Glomerulonephritis	c-16627
6	Female-spayed, Mixed breed, 6 years.	779	Glomerulonephritis	c-3020
7	Male-neutered, Schnauzer, 10 years.	855	Glomerulonephritis	c-1856
8	Female, Rottweiler, 4 years.	573	Glomerulonephritis	c-3214
9	Female-spayed, Terrier, 4 years.	1036	Glomerulonephritis	c-1586
10	Male-neutered, Shetland Shepherd, 5 years.	110	Glomerulonephritis	c-8499
11	Male-neutered, Mixed, 6 years.	538	Glomerulonephritis	c-16052

Table VIII. Amyloidosis group (3 cases)

Case No.	Signalment	Serum creatinine concentration (µmol/L)	Postmortem pathological diagnosis	Lab. No.
1	Female-spayed, Shar pei, N/A	1205	Amyloidosis	c-20719
2	Female-spayed, Shar pei, 8 years.	351	Amyloidosis	c-20965
3	Female-spayed, English Setter, 14 years.	130	Amyloidosis	c-12317

Table IX. Nephrocalcinosis (1 case)

Case No.	Signalment	Serum creatinine concentration (µmol/L)	Postmortem pathological diagnosis	Lab. No.
1	Female, Labrador Retriever, 5 years.	350	Nephrocalcinosis	c-11827

Table X. Granulomatous nephritis (1 case)

Case No.	Signalment	Serum creatinine concentration (µmol/L)	Postmortem pathological diagnosis	Lab. No.
1	Female-spayed, 2 years.	444	Granulomatous nephritis	c-239

Table XI. Volume fraction of renal cortical structures (descriptive statistics)

Groups analyzed	Variables observed (mean ± 1 standard deviation)				
(n= number of cases per group)	serum creatinine concentration (μmol/L, mean ±1SD)	interstitial volume fraction ($intV_V$)	tubular volume fraction ($tubV_V$)	capillary volume fraction ($capV_V$)	glomerular volume fraction ($glomV_V$)
Control, n=5	78 ±16	0.1920 ±0.0346	0.7378 ±0.0449	0.0063 ±0.0048	0.0649 ±0.0392
Chronic interstitial nephritis, n=18	329 ±299	0.4059 ±0.1328	0.5121 ±0.1579	0.0081 ±0.0079	0.0756 ±0.0693
Glomerulonephritis, n=11	469 ±336	0.4020 ±0.1462	0.4671 ±0.0942	0.0139 ±0.0233	0.1172 ±0.0802
Amyloidosis, n=3	562 ±567	0.4600 ±0.0826	0.4193 ±0.1295	0.0098 ±0.0044	0.1096 ±0.0772
Nephrocalcinosis, n=1	350	0.4178	0.5333	0.0010	0.0489
Granulomatous Nephritis, n=1	444	0.7867	0.1733	0.0010	0.0400

Table XII. Morphometry of the glomeruli (descriptive statistics)

Groups analyzed (n= number of cases per group)	Variables observed (mean ± 1 standard deviation)					
	Serum creatinine concentration (µmol/L)	Glomerular area (µm²) (glomA)	Glomerular tuft area (µm²) (tuftA)	Bowman's space area (µm²) (bwsA)	Bowman's capsule harmonic thickness (µm) (harT)	Volume weighted mean volume of glomeruli (µm³) (vwmvg)
Control, n=5	78 ±16	24362 ±4706	15873 ±3614	8489 ±2036	2.0944 ±0.260	3828317 ±1322964
Chronic interstitial nephritis, n=18	329 ±299	30093 ±1213	13931 ±4187	16169 ±1077	3.602 ±1.075	5521856 ±3068483
Glomerulonephritis, n=11	469 ±336	36211 ±1794	15593 ±7508	20618 ±1377	4.893 ±1.663	7657599 ±5888838
Amyloidosis, n=3	562 ±567	33779 ±9698	16389 ±6009	17389 ±5124	3.138 ±0.527	4650267 ±1818915
Nephrocalcinosis, n=1	350	40959	17985	22973	4.767	7612460
Granulomatous Nephritis, n=1	444	15150	9498	5652	3.210	2282623

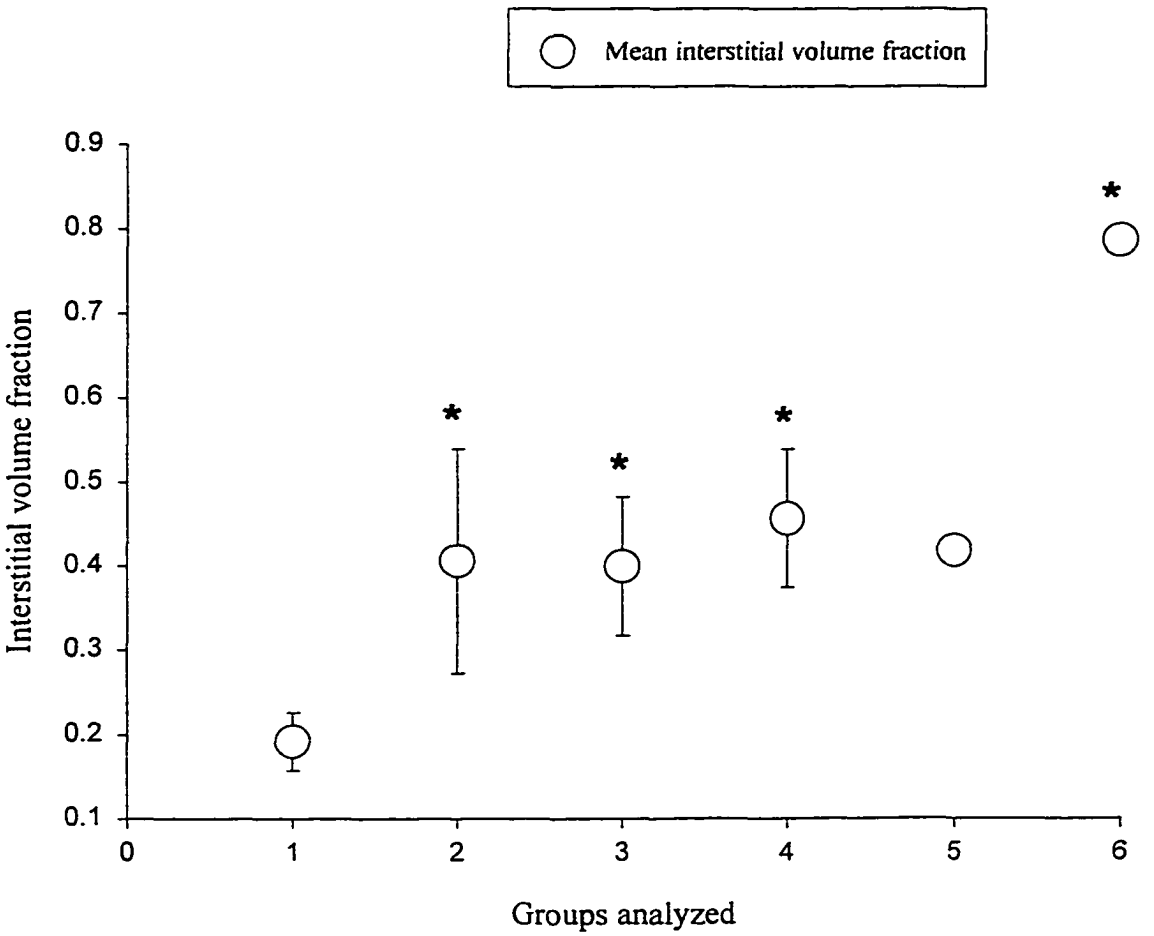

Figure 7. Mean interstitial volume fraction per histopathological group: control (1), chronic interstitial nephritis (2), glomerulonephritis (3), amyloidosis (4), nephrocalcinosis (5), granulomatous nephritis (6). Asterisks indicate groups that are significantly greater than control.

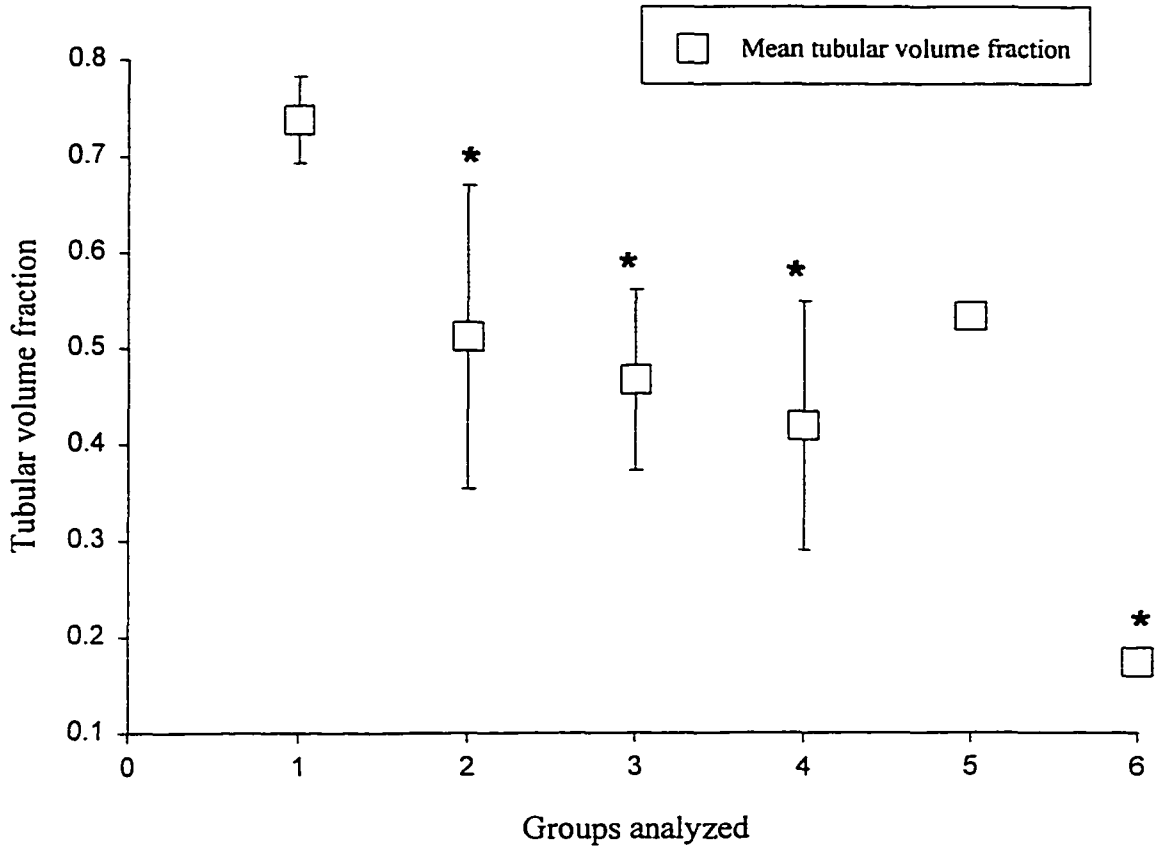

Figure 8. Mean tubular volume fraction per histopathological groups: control (1), chronic interstitial nephritis (2), glomerulonephritis (3), amyloidosis (4), nephrocalcinosis (5), granulomatous nephritis (6). Asterisks indicate groups that are significantly less than control.

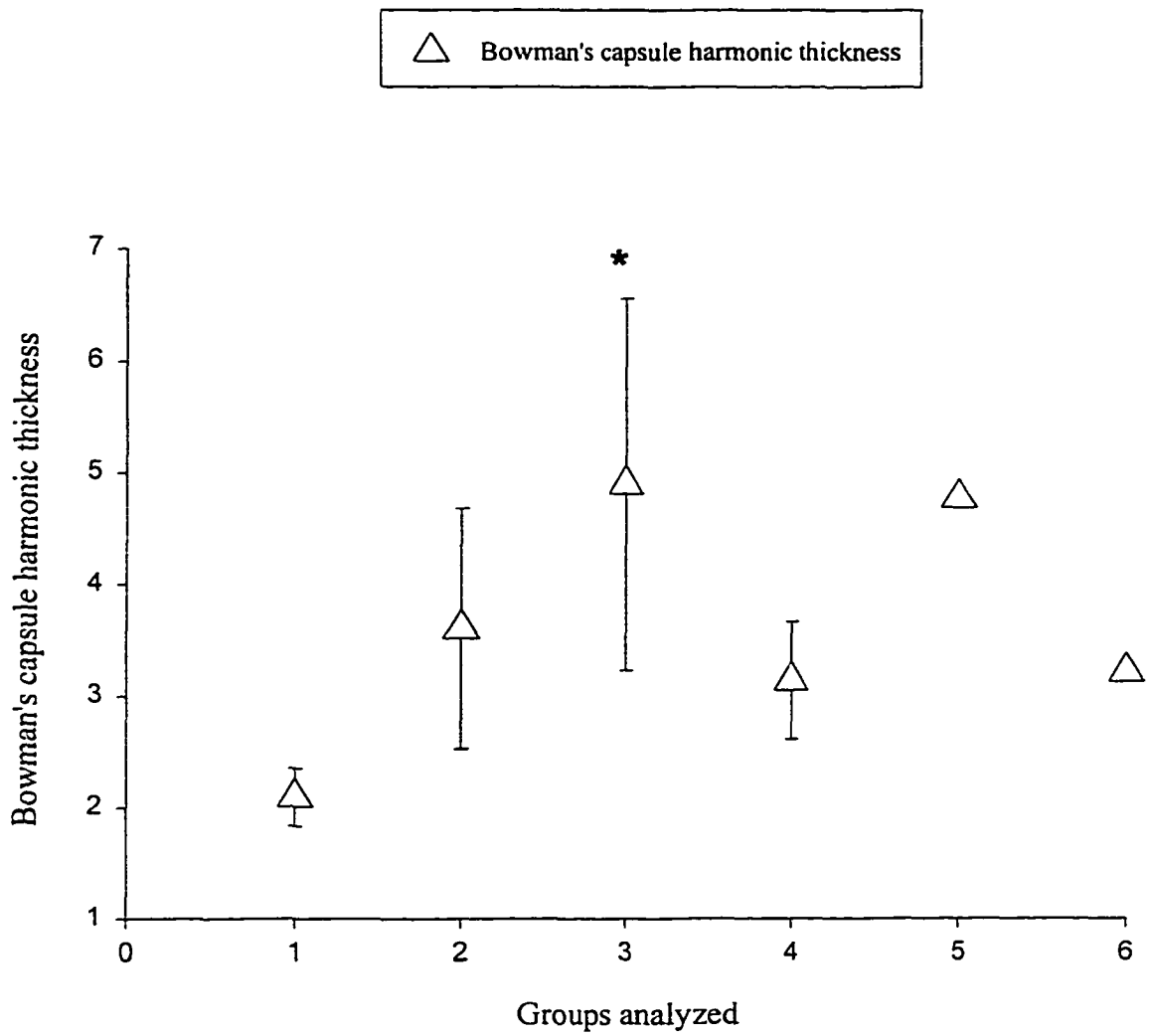

Figure 9. Mean Bowman's capsule harmonic thickness per histopathological group: control (1), chronic interstitial nephritis (2), glomerulonephritis (3), amyloidosis (4), nephrocalcinosis (5), granulomatous nephritis (6). Asterisks indicate group that is significantly greater than control.

Table XIII. Association between serum creatinine concentration and measured cortico-renal variables.
(main study n=39)

Variables analyzed	Serum creatinine concentration		
	Correlation coefficient		P values
Interstitial volume fraction	r^2=33.6%	r=0.58*	P=0.00
Tubular volume fraction	r^2=31.3%	r=-0.56*	P=0.00
Capillary volume fraction	r^2=3.6%	r=0.19	P=0.23
Glomerular volume fraction	r^2=.36%	r=0.06	P=0.68
Glomerular area	r^2=16%	r=0.40*	P=0.01
Glomerular tuft area	r^2=.16%	r=-0.04	P=0.77
Bowman's space area	r^2=26%	r=0.51*	P=0.01
Bowman's capsule harmonic mean thickness	r^2=20.2%	r=0.45*	P=0.004
Volume weighted mean volume of glomerulus	r^2=10.9%	r=0.33*	P=0.04

*Significant correlation coefficient

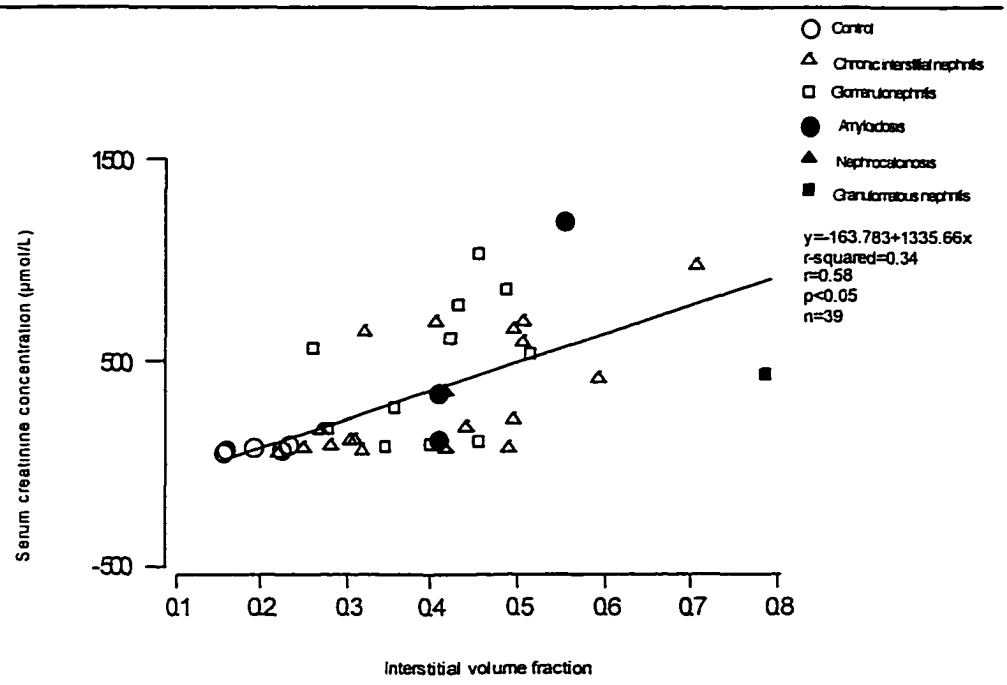

Figure 10. Correlation between serum creatinine concentration and interstitial volume fraction. An increase in interstitial volume fraction is accompanied by a significant increase in serum creatinine concentration.

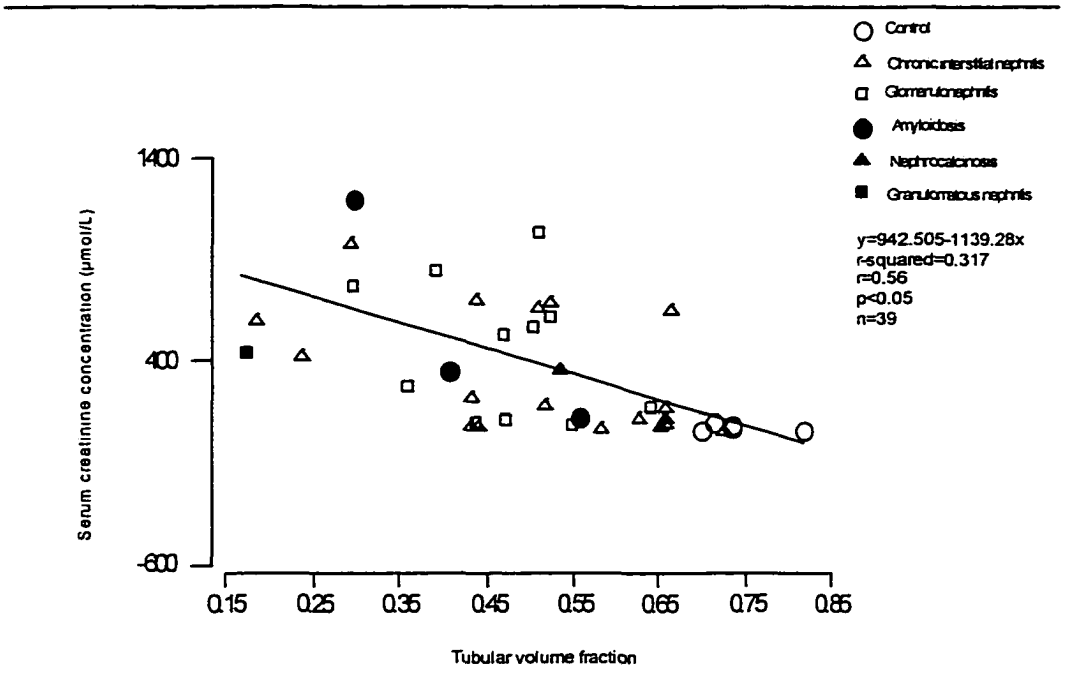

Figure 11. Correlation between serum creatinine concentration and tubular volume fraction. An decrease in tubular volume fraction is accompanied by a significant increase in serum creatinine concentration

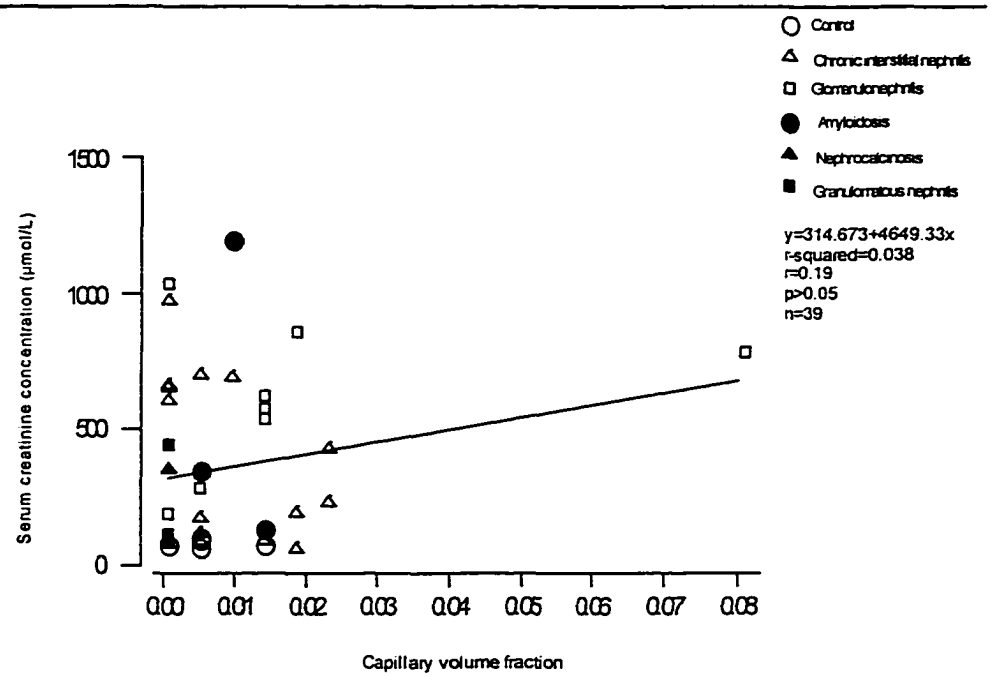

Figure 12. Correlation between serum creatinine concentration and capillary volume fraction. There was no significant correlation between serum creatinine concentration and capillary volume fraction

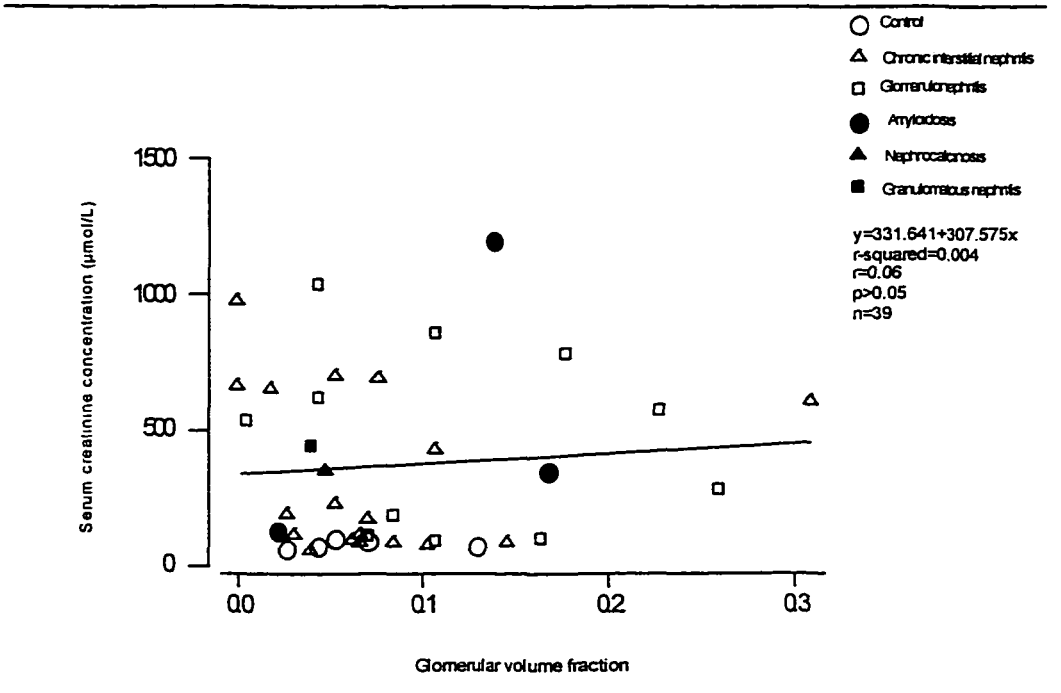

Figure 13. Correlation between serum creatinine concentration and glomerular volume fraction. There was no significant correlation between serum creatinine concentration and glomerular volume fraction.

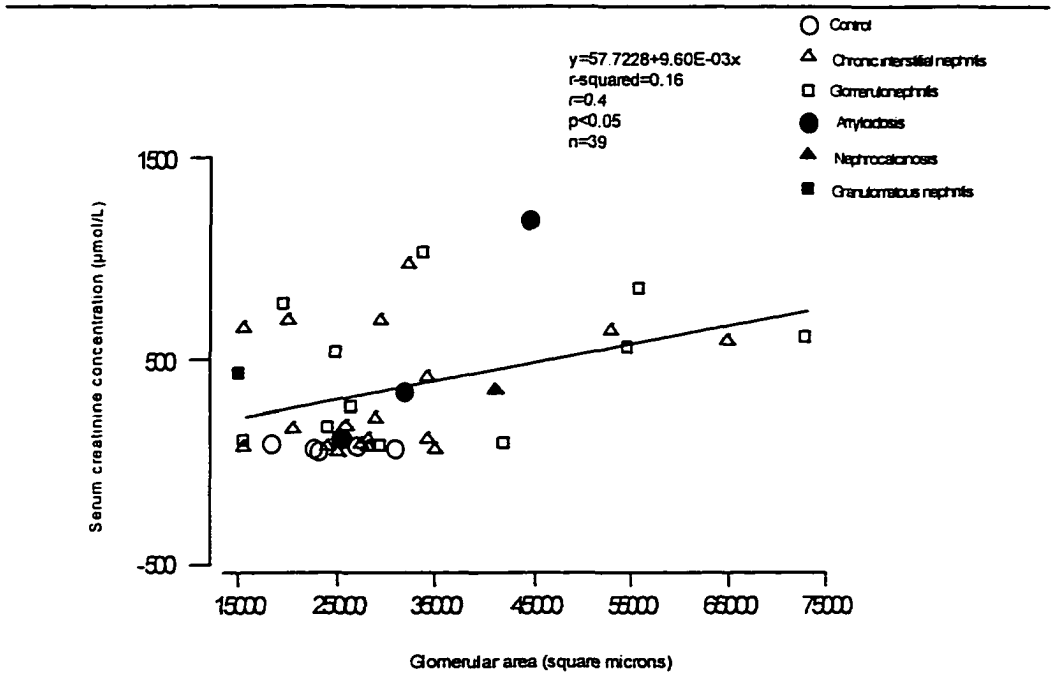

Figure 14. Correlation between serum creatinine concentration and glomerular area. An increase in glomerular area is accompanied by a significant increase in serum creatinine concentration.

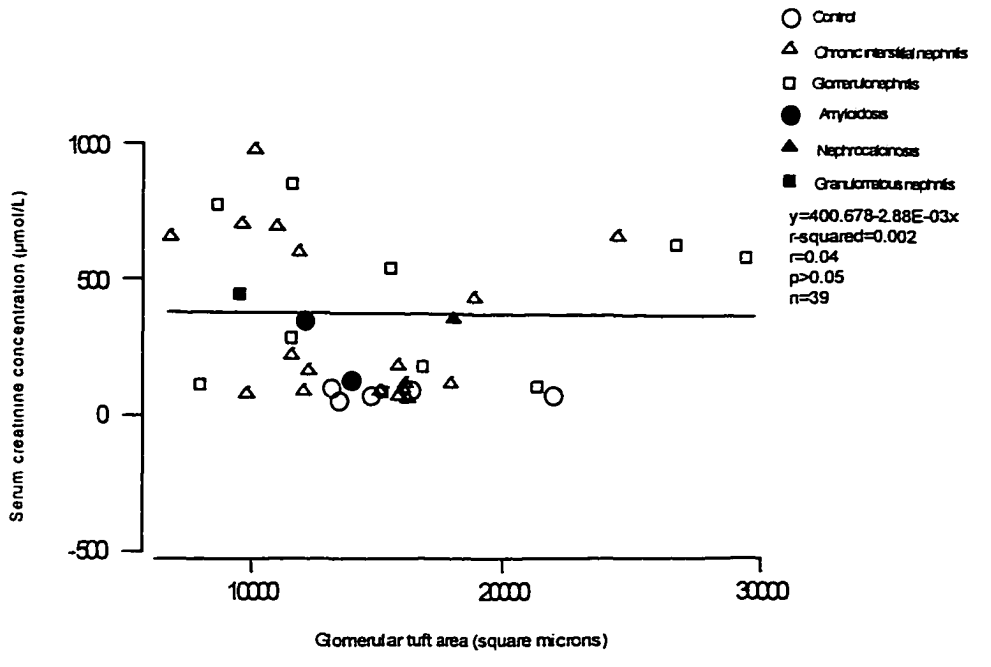

Figure 15. Correlation between serum creatinine concentration and glomerular tuft area. There was no correlation between serum creatinine concentration and glomerular tuft area.

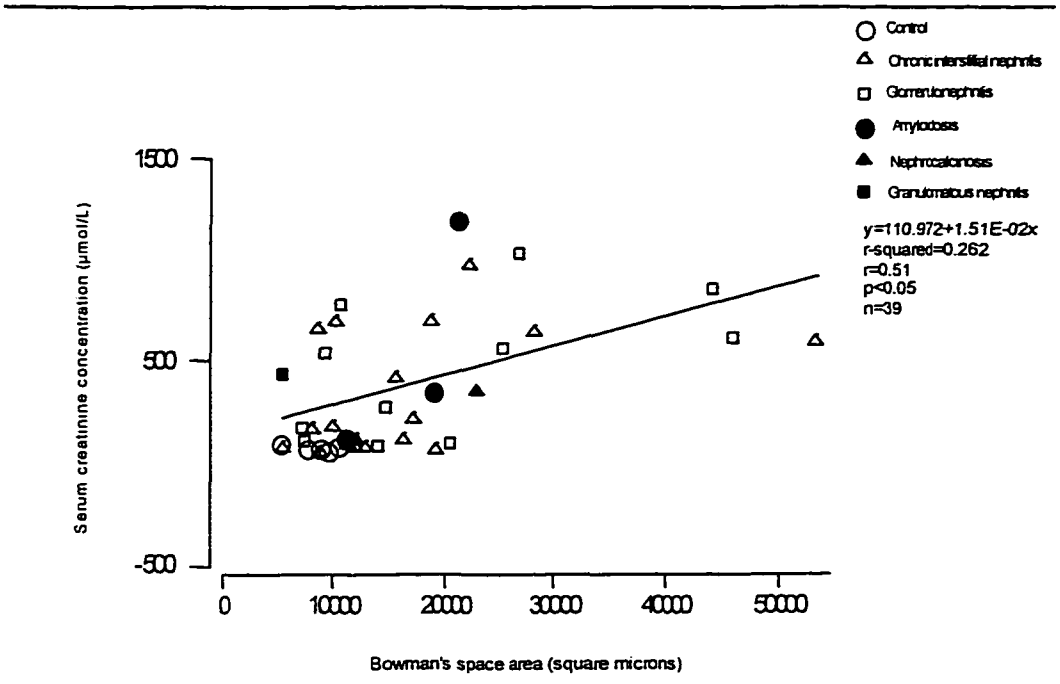

Figure 16. Correlation between serum creatinine concentration and Bowman's space area. An increase in Bowman's space area is accompanied by a significant increase in serum creatitnine concentration.

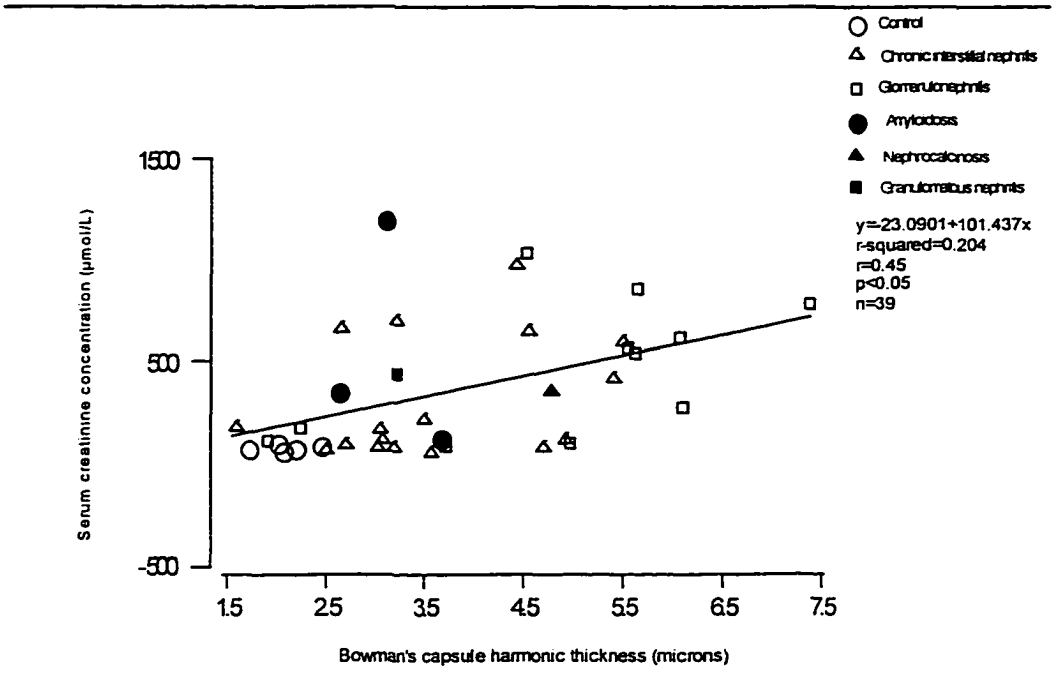

Figure 17. Correlation between serum creatinine concentration and Bowman's capsule harmonic thickness. An increase in Bowman's capsule harmonic thickness is accompanied by a significant increase in serum creatinine concentration.

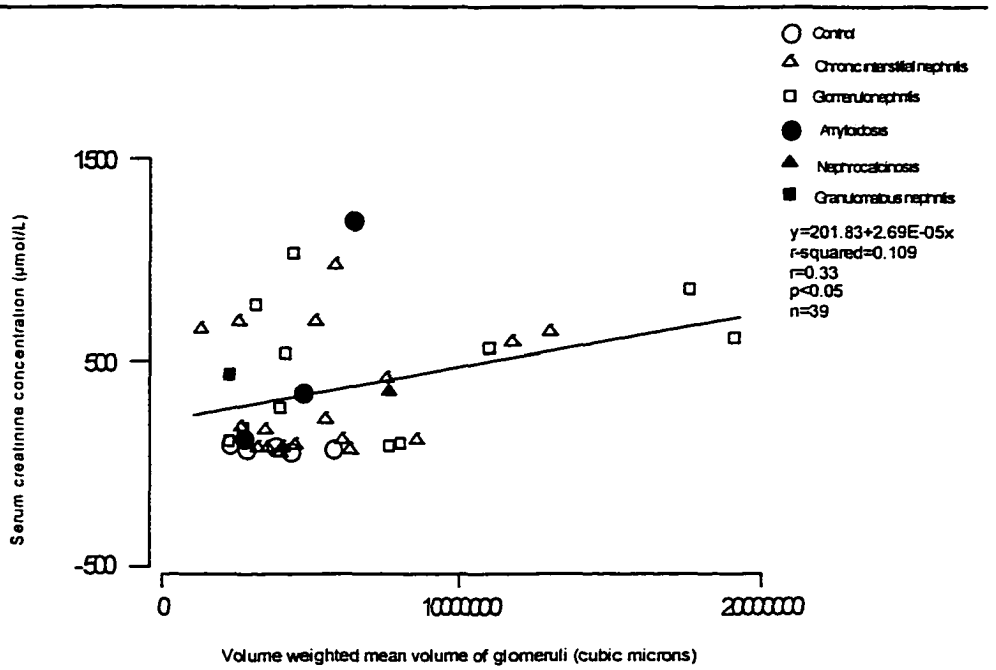

Figure 18. Correlation between serum creatinine concentration and volume weighted mean volume of the glomeruli. An increase in volume weighted mean volume of the glomeruli is accompanied by a significant increase in serum creatinine concentration.

2.3.3. Discussion

In order to evaluate the relationship between structural abnormalities and renal function in dogs with different naturally occurring renal diseases, standardization of structural measurements and histopathological examination of cases was necessary. However, the discussion will mostly consider the groups that were composed of more than one case such as control, chronic interstitial nephritis, glomerulonephritis, and amyloidosis. Because there was only one case each of nephrocalcinosis and granulomatous nephritis, the data was analyzed together with all of the cases (n=39). The structural alterations in these two cases were similar to those in the other disease groups.

Four basic renal structures were measured morophometrically (interstitium, tubules, capillaries and glomeruli). Most of the measurements were related to the glomerulus (glomerular volume fraction, glomerular area, glomerular tuft area, Bowman's space area, Bowman's capsule harmonic thickness, and volume weighted mean volume of the glomeruli). Despite several glomerular alterations, few measurements were statistically different from control and most had a lower correlation coefficient to serum creatinine concentration as compared to tubulointerstitial measurements. Analysis of variance demonstrated significant differences for interstitial volume fraction, tubular volume fraction and Bowman's capsule harmonic thickness. In addition, multiple comparison analysis between the control group and disease groups demonstrated that: 1) interstitial and tubular volume fraction increased and decreased, respectively, in chronic interstitial nephritis, glomerulonephritis, amyloidosis, and granulomatous nephritis; and 2) Bowman's capsule harmonic thickness was increased significantly only in glomerulonephritis. When interstitial

volume fraction was increased, the tubular volume fraction was significantly decreased. Analysis of covariance showed that the absolute volume of kidney/nephron occupied by interstitium had a significant tendency to increase with increasing creatinine levels. The absolute volume of kidney/nephron occupied by tubules remains the same and does not change either with different serum creatinine concentrations or with different disease groups. It is possible that when glomeruli dropout, the nephrons disappear and the empty area is filled by interstitial proliferation and the remaining functional nephrons maintain their absolute tubular volume. If tubular hypertrophy occurs this is not morphometrically significant. Glomerular and capillary volume fraction did not change significantly. When interstitial volume is increased (wider), it may contribute to decreasing intertubular capillary area and compromise blood flow(32). If blood flow is diminished, the supply of oxygen and nutrients to the tubules is reduced leading to tubular atrophy. Tubular atrophy may lead to the formation of atubular glomeruli (15). Atubular glomeruli may cause a decreased filtration rate since blood does not get filtered. Also, if tubular epithelial cells are damaged, tubular sodium chloride reabsorption is decreased leading to an increased delivery of NaCl to the macula densa and to a reduction in renin-angiotensin system activity (tubuloglomerular feed back)(46). This results in dilatation of the afferent and efferent arterioles (51) and reduction in glomerular filtration rate. In addition, glomerular filtration rate may be reduced by obstruction (due to fibrosis) of postglomerular capillaries. This could lead to a rise in hydrostatic pressure and to a reduction in glomerular blood flow and therefore to a rise in serum creatinine concentration (31). In our study, widening of the renal cortical interstitium (increased interstitial volume fraction) was accompanied by a significant increase in serum

creatinine concentration and a significant decrease in tubular volume fraction. The decrease in tubular volume fraction implies a decrease in functional tubular cells and a decrease in tubular reabsorption/secretion. Moreover, this process leads to a decrease in total functional renal mass. Our findings suggest that tubulointerstitial alterations (interstitial and tubular volume fraction) had more functional impact on renal function than glomerular alterations.

Pearson correlation showed there was a stronger correlation between serum creatinine concentration and interstitial volume fraction or tubular volume fraction as compared to glomerular area, Bowman's space area, Bowman's capsule harmonic thickness, and volume weighted mean volume of the glomeruli. Therefore this suggest that interstitial volume fraction and tubular volume fraction have more effect on serum creatinine concentration.

Multiple regression was performed in order to determine which variables accounted for the majority of the variation in serum creatinine concentration. Serum creatinine concentration as a dependent variable was introduced in the multiple regression model because this was used as an indicator of renal function. Interstitial volume fraction and glomerular area were chosen according to the high correlation coefficient, and the most reliable glomerular measurement, respectively. In addition, standardization of the resulting equation was performed to establish which independent variable had a greater influence on serum creatinine concentration. The multiple regression equation had a squared multiple correlation coefficient (R^2) of 48%, meaning that 48% of the serum creatinine concentration variation is explained by interstitial volume fraction and glomerular area. By examining the standardized equation, interstitial volume fraction has about 1.5 times (184/122) the influence on serum creatinine concentration than does glomerular area.

The result of this study were similar to comparable investigations in human beings. Our results showed a correlation coefficient of r=0.58 between interstitial volume fraction and serum creatinine concentration. In human beings, correlation coefficients between interstitial volume fraction and serum creatinine concentration have been reported as r=0.64 (glomerulonephritis, n=67) (6), r=0.75 (amyloidosis, n=48)(30), and r=0.85 (glomerulosclerosis, n=57)(6). The correlation coefficients were somewhat higher than in our study. This could be because those studies examined specific renal diseases, whereas our study included several different renal diseases. In addition, the number of cases in our study was less than those in the studies from human beings. Furthermore, our study, as in the studies from human beings, demonstrated that glomerular alterations are not as strongly associated with decreased renal function as are tubulointerstitial alterations.

As a sequela of inflammation and injury, different cytokines (TGF-β, PDGF) elaborated by circulating mononuclear inflammatory cells recruited into the inflammatory site may activate fibrogenic responses in resident tubular and interstitial cells (e.g. fibroblast). These processes stimulate kidney tissue to produce extracellular matrix molecules, like collagen, fibronectin and proteoglycans (4). Overproduction of all these factors generate fibrosis.

It is important to know if glomerular or tubulointerstitial damage has more impact on renal function because this may identify specific therapeutic strategies in dogs with renal disease. The results of this study would suggest that therapies which reduce interstitial inflammation and fibrosis would preserve or improve renal function more than therapies directed at glomerular abnormalities.

3. IDENTIFICATION OF THE SUBSETS OF INFILTRATING MONONUCLEAR INFLAMMATORY CELLS IN THE RENAL INTERSTITIUM

3.1. Introduction

Infiltrating mononuclear inflammatory cells in the renal interstitium such as T-lymphocytes play an important role in the initiation and progression of renal pathology (e.g. tubulointerstitial fibrosis) in animals and human beings. Some nephritogenic antigens are derived from renal cells (e.g. tubular epithelial cells) and their extracellular structures, and others are extrarenal antigens added to the microenvironment from the circulation (52). Renal tubular epithelial cells may contribute to immune responses since they can be induced to express surface molecules (e.g. adhesion molecules) or secrete cytokines which facilitate engagement with T lymphocytes (53). Progressive inflamation or injury to the renal interstitium can destroy extensive amounts of renal tissue and may considerably decrease renal function (e.g. glomerular filtration, tubular reabsorption and secretion). A significant portion of the inflammatory process is immunologic in nature. Mononuclear infiltrates release cytokines (interleukin-1, transforming growth factor-α), which collectively create a microenvironment which impairs function and alters structure (e.g. fibrosis, extracellular matrix expansion) (52). Studies in human beings show that primary or secondary interstitial nephritidities are initially characterized by the presence of mononuclear infiltrates with the majority being T lymphocytes (15). The predominance of $CD4^+$ or $CD8^+$ T-lymphocytes

depends on the underlying cause. $CD4^+$ lymphocytes may influence fibroblast and epithelial cells via the release of cytokines and $CD8^+$ lymphocytes are directly cytotoxic to tubulointerstitial cells bearing their target antigen (15). Both cell types may lead directly or indirectly to the induction of tubulointerstitial fibrosis . In dogs with naturally occurring renal disease, the identity of the infiltrating lymphocytes has not been previously determined. Immunohistochemical techniques allow the identification of lymphocytes and other cells. An avidin-biotin immunohistochemical method was used to identify T-lymphocyte subsets in diseased canine renal tissue. The identification of inflammatory cells which infiltrate into the renal interstitium will contribute to the understanding of the pathogenesis of renal failure in dogs.

3.2. Materials and Methods

Infiltrating mononuclear inflammatory cells in the renal interstitium were analyzed in frozen kidney tissue from eleven dogs with different forms of naturally occurring renal disease. Tissue sections from histologically normal kidney and mesenteric lymph node from three dogs were used as a negative and positive controls, respectively.

3.2.1. Sample collection and snap freezing

Kidney tissue was collected from 11 dogs with clinical and serum biochemical evidence of renal disease who died or were euthanized at the Atlantic Veterinary College Teaching Hospital. Samples were collected within 12 hours of death. Normal kidney and mesenteric lymph node tissue were obtained from three, recently euthanized dogs from the

local humane animal shelter. Tissue, was rapidly frozen by placing it on small cork mats (1.5 x 1.5 cm) and repeatedly immersing it in precooled (in liquid nitrogen) isopentane (2-Methyl-butane)(54). The frozen tissues were placed in a precooled polyethylene bags and stored at -82°C.

3.2.2. Cryostat Sections and Fixation

Four tissue sections, five micron thick, from the frozen tissue were obtained for each of the 11 cases by cutting them in a cryostat (Leitz Kryostat 1720, Leica, Inc., USA). The Cryostat is a microtome housed in a refrigerated cabinet with a regulated temperature between zero and -30°C. Tissue was sectioned at approximately -22°C. Adjacent tissue sections from the clinical cases and tissue sections from normal kidney and lymph node (negative and positive controls, respectively) were cut. Tissue sections were placed on glass slides which had been pre-treated with the adhesive aminoalkylsilane. The samples were air dried followed by fixation in cold acetone for five minutes. Fixing sections in cold acetone prevents detachment from the slide and preserves morphologic details (54). Immunohistochemical staining was performed the same day the sections were cut.

3.2.3. Immunohistochemical principles

As previously discussed, immunohistochemistry (IHC) is a specific staining technique. Avidin-biotin complex (ABC) is an enzymatic IHC method which utilizes the high affinity of avidin (a high molecular weight glycoprotein) for biotin (a low molecular weight vitamin)(33). Avidin is bound to biotin which is coupled to a horseradish peroxidase

reporter molecule to form a complex. The avidin in the complex still has unoccupied receptors for binding to the biotinylated secondary antibody therefore the staining is amplified. Rat anti-canine monoclonal antibodies to $CD4^+$ and $CD8^+$ antigens were used for immunohistochemical staining. Monoclonal antibodies are produced by clones of plasma cells. Antibodies from a given clone are immunochemically identical and react with a specific epitope on the antigen against which they are raised (35). Advantages of monoclonal antibodies are high homogeneity and the absence of nonspecific antibodies (35).

3.2.4. Immunohistochemical staining procedure

Renal interstitial infiltration of $CD4^+$ and $CD8^+$ T-lymphocytes was identified by the indirect immunoenzyme ABC method (Figure 19). The sequence of reagent application was primary antibody, biotinilated secondary antibody, preformed avidin-biotin-enzyme complex and, substrate solution. Enzymatic activity produces a visible color change in a substrate at the sites of antibody-enzyme-complex deposition within the tissue. Rat monoclonal antibodies against canine $CD4^+$ and $CD8^+$ lymphocyte cell surface antigens (Serotec Ltd., Raleigh, NC) were used in conjunction with an avidin-biotin complex (ABC) technique. The primary antibodies (rat anti-canine $CD4^+$ and rat anti-canine $CD8^+$) were diluted to a concentration of 1:100 in 1.5% normal rabbit serum. Normal rabbit serum (NRS) was used to avoid adsorption of the antibody to the plastic container in which the final dilution was made. Appropriate dilution of each monoclonal antibody and the staining procedure were determined by preliminary stains performed on normal canine mesenteric lymph node tissue. Vectastain® ABC solutions (Vector Lab. Inc. Burlingame, CA) (i.e., normal rabbit serum,

rabbit anti-rat biotilynated secondary antibody and ABC reagent) were prepared according to Vectastain® ABC kit instructions at room temperature. Reagents were applied to the tissue sections and incubated in a humidity chamber at room temperature (20°C). The sequence of steps were as follows:

1) Apply phosphate buffered saline (PBS). Incubate for five minutes.

2) Apply PBS containing 1.5 % NRS. Incubate for 20 minutes.

3) Blot excess serum.

4) Apply rat anti-canine $CD4^+$ or $CD8^+$ monoclonal antibody (1:100 dilution; each on their corresponding tissue section). Incubate for one hour.

5) Apply PBS. Incubate for 10 minutes.

6) Apply rabbit anti-rat biotinylated antibody. Incubate for 30 minutes.

7) Apply PBS. Incubate for 10 minutes.

8) For suppression of endogenous peroxidase activity, apply 0.3% hydrogen peroxide. Incubate for 20 minutes.

9) Apply PBS. Incubate for 10 minutes.

10) Apply avidin-biotin complex reagent. Incubate for 45 minutes.

11) Apply PBS. Incubate for 10 minutes.

12) Apply diaminobenzidine (DAB) substrate (Sigma, St. Louis, Mo., consisted of 18 ml of PBS, 7 μL of 30% hydrogen peroxide and 10 mg 3,3'-diaminobenzidine); Incubate for four to four and half minutes and then rinse with tap water.

Slides were counterstained with aqueous 4.7% hematoxylin for one second. Slides were mounted with Flo-tex mounting medium (Lerner Lab., Pittsburgh, PA) and examined

with a light microscope (Carl Zeiss, Canada Ltd., Don Mills, ON).

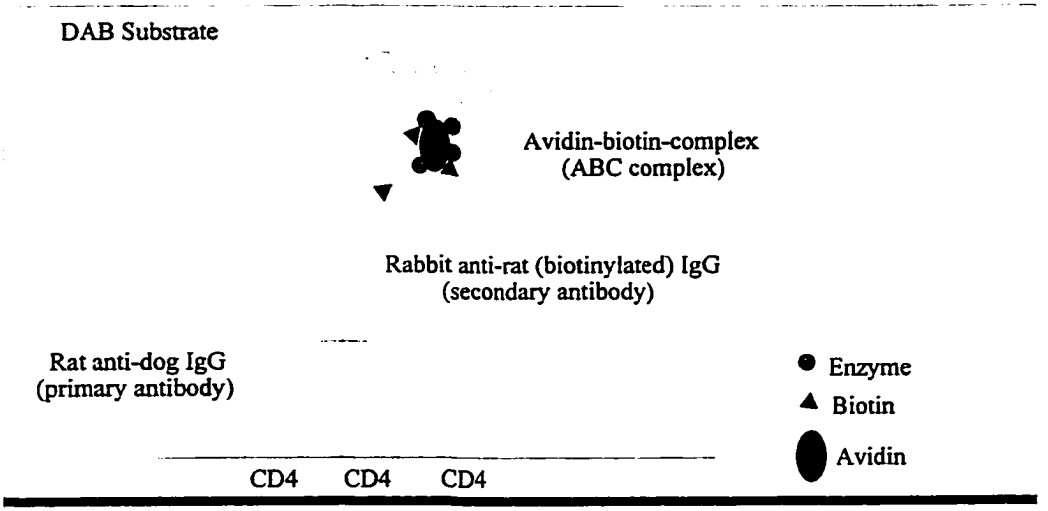

Figure 19. Indirect (sandwich) immunohistochemical method utilizing the avidin-biotin-complex. The primary antibody is unlabeled. The method utilizes a labeled secondary antibody which has specificity against the primary antibody.

3.2.5. Tissue controls

Reagent and procedure controls are necessary for the validation of immunohistochemical staining results. Specificity of labeling was evaluated by substitution of PBS for the primary monoclonal antibody in the deletion control sections. Cross reaction of the primary antibodies with non $CD4^+$ or $CD8^+$ antigens was assessed using a normal kidney tissue control. Normal mesenteric lymph node tissue was used as a positive control to verify binding with the $CD4^+$ and $CD8^+$ antigen. The positive control validates the staining procedure (and all the reagents) and also confirms the preservation of the antigen under investigation. The negative control tissue (normal kidney tissue) lacked the antigen under study. The absence of pathologic alteration in the normal kidney and lymph node tissue was confirmed by histopathologic examination.

3.2.6. Field selection, cell localization and quantification

3.2.6.1. Field selection

Four adjacent tissue sections (two per slide) were used for each of the 11 cases, one section was stained for $CD4^+$, the other for $CD8^+$ and the remaining two sections were used as deletion (primary antibody was not applied) controls. From each tissue section, fields were randomly selected by using a 26 x 76 mm plastic grid (same size as the microscope slide) with 533 points. The total number of points that contacted the histological section were counted and multiplied by a number chosen from a random number table. The resulting value was the field number and this was demarcated with a marker.

3.2.6.2. Cell localization and quantification

Using 400 diameters magnification (40X) at the light microscopic level, each randomly selected (demarcated) field was brought into focus and the demarcated field was erased from the slide to count T-lymphocytes. Six, 32,500 μ^2 fields per tissue section were evaluated for $CD4^+$ or $CD8^+$ cells. The total cross sectional area evaluated was 195,000 μ^2 per tissue section. Positive staining of $CD4^+$ and $CD8^+$ lymphocytes was observed when a brown color (Figure 20-21) was detected within a cell, while no brown stain was observed in negative control tissue (Figure 22). The resulting data were recorded in a Minitab worksheet for statistical analysis.

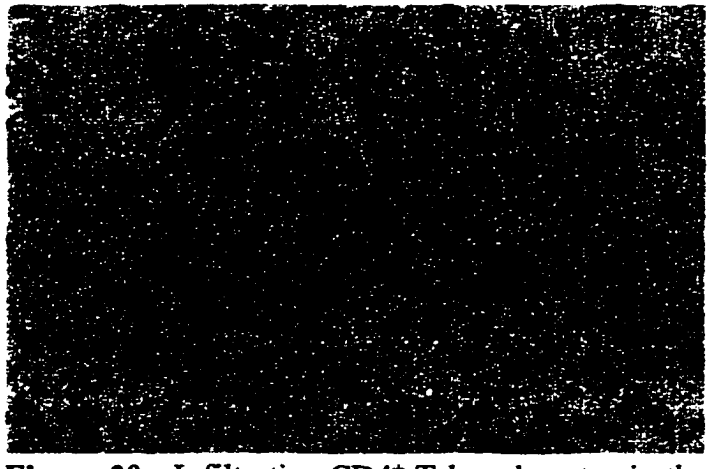

Figure 20. Infiltrating $CD4^+$ T-lymphocytes in the renal interstitium. DAB peroxidase substrate imparts a brown color to positively staining cells. (250 X, Hematoxylin counterstain).

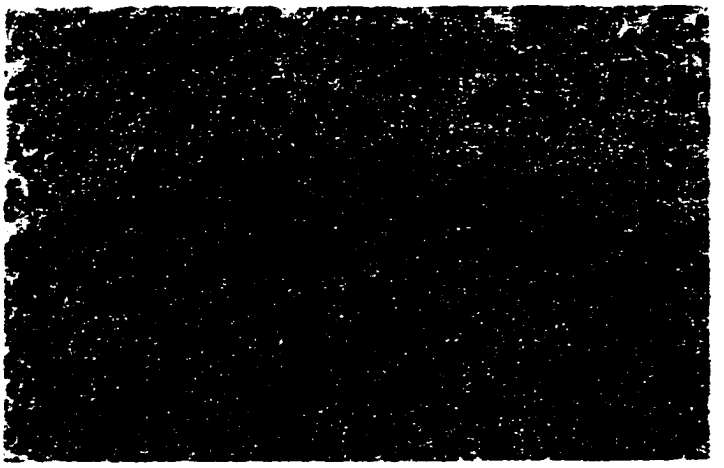

Figure 21. $CD4^+$ T-lymphocytes in mesenteric lymph node. DAB peroxidase substrate imparts a brown color to positively staining cells. (250 X, Hematoxylin counterstain).

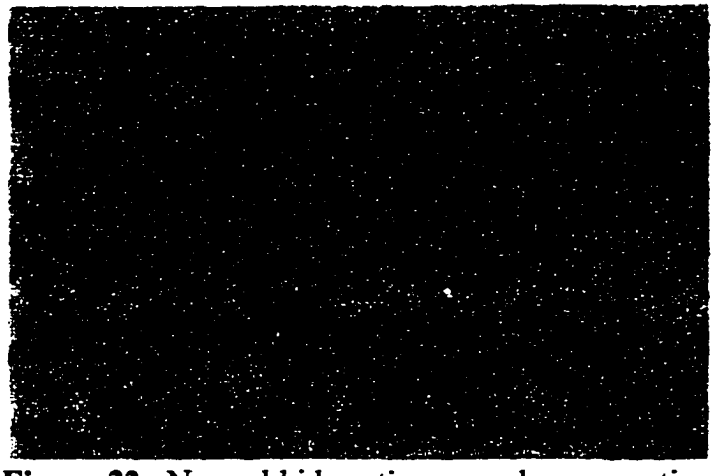

Figure 22. Normal kidney tissue used as a negative control. No brown stain was observed. (250 X, Hematoxylin counterstain).

3.2.7. Histopathological categorization

Tissue sections were examined histopathologically and grouped (control, mild, moderate, severe) according to the degree of glomerular and tubulointerstitial inflammatory cell infiltration and interstitial fibrosis. Categorization was preformed separately by two pathologists who had no knowledge of the lymphocyte counts.

3.2.8. Statistical analysis

Using Minitab® (1994, Minitab Inc., State college PA), descriptive statistics on $CD4^+$ and $CD8^+$ T-lymphocyte numbers were obtained for each histopathological group.

Since the data consisted of small numbers (0-27 cells/case), statistical analysis was best accomplished by taking the square root of each observation before proceeding (55). When very small values are involved, the square root overcorrects so that the range of transformed values giving a small mean may be larger than the range of transformed values giving a larger mean. For this reason, the addition of 0.5 to each value followed by square rooting it is recommended as an appropriate transformation when some values are under 10 and especially when zeros are present (55).

After transforming the data, a one way analysis of variance was used to compare data within and among histopathological groups.

Dunnett's test multiple comparison was applied to determine if statistically significant differences existed between the control group and disease groups.

A P value equal or less than 0.05 was considered significant.

3.3. Results

Four histopathological groups were identified according to the degree of glomerular and tubulointerstitial inflammatory cell infiltration and interstitial fibrosis from the 14 cases: control (3 cases); mild (3 cases); moderate (4 cases); and severe (4 cases).

Histological examination of normal kidney (negative control) and lymph node (positive control) did not reveal abnormalities. Tissue sections from normal kidney had no T-lymphocyte infiltration. Tissue sections from two cases in the moderate and from one case in the severe group had no infiltration of $CD8^+$ T-lymphocytes. Tissue sections from all other cases had varying proportions of infiltrating $CD4^+$ and $CD8^+$ T-lymphocytes. Cell numbers/field in each of the six fields per case are reported in table XIV. Serum creatinine concentration was not available (NA) in the control group and from one case in the moderate group.

The average number, before transformation, of $CD4^+$ and $CD8^+$ T-lymphocytes per histopathological group is reported in table XV. The data was transformed for statistical purposes and is reported as an average ± 1 standard deviation (Table XVI).

One way analysis of variance revealed that the proportion of $CD4^+$ versus $CD8^+$ T-lymphocytes between the disease groups (Figure 23) was not statistically different (mild group P=0.4, moderate group P=0.9, severe group P=0.7). A statistically significant difference was found in the total average number of $CD4^+$ and $CD8^+$ (analyzed together because they were not different in proportion) cells between groups (P=0.007). The multiple comparison Dunnett's test showed that the severe group but not the mild and moderate group was statistically different (greater) than the control group (Figure 24).

Table XIV. Quantification of $CD4^+$ and $CD8^+$ T-lymphocytes*.

Group under observation**	Field No.	$CD4^+$ No.	$CD8^+$ No.	Serum creatinine concentration (μmol/L)	Group under observation**	Field No.	$CD4^+$ No.	$CD8^+$ No.	Serum creatinine concentration (μmol/L)
Control	1	0	0	NA	Mild	1	3	7	140
	2	0	0	NA		2	0	3	140
	3	0	0	NA		3	0	0	140
	4	0	0	NA		4	0	0	140
	5	0	0	NA		5	0	0	140
	6	0	0	NA		6	0	0	140
Control	1	0	0	NA	Mild	1	0	2	351
	2	0	0	NA		2	1	0	351
	3	0	0	NA		3	1	0	351
	4	0	0	NA		4	1	0	351
	5	0	0	NA		5	1	0	351
	6	0	0	NA		6	0	0	351
Control	1	0	0	NA	Mild	1	0	0	664
	2	0	0	NA		2	0	0	664
	3	0	0	NA		3	0	0	664
	4	0	0	NA		4	0	2	664
	5	0	0	NA		5	2	2	664
	6	0	0	NA		6	2	2	664
Moderate	1	5	2	NA	Severe	1	2	2	424
	2	1	0	NA		2	5	10	424
	3	0	1	NA		3	6	6	424
	4	0	1	NA		4	2	7	424
	5	0	0	NA		5	1	13	424
	6	0	0	NA		6	13	3	424
Moderate	1	0	0	353	Severe	1	0	0	976
	2	2	0	353		2	1	0	976
	3	4	0	353		3	0	0	976
	4	1	0	353		4	0	0	976
	5	5	0	353		5	0	0	976
	6	11	0	353		6	2	0	976
Moderate	1	0	0	1032	Severe	1	0	3	292
	2	1	0	1032		2	6	27	292
	3	0	0	1032		3	3	12	292
	4	0	0	1032		4	0	15	292
	5	0	0	1032		5	5	3	292
	6	2	0	1032		6	5	2	292
Moderate	1	1	7	645	Severe	1	4	3	1205
	2	1	4	645		2	2	1	1205
	3	1	3	645		3	3	1	1205
	4	0	1	645		4	3	0	1205
	5	0	4	645		5	2	0	1205
	6	0	1	645		6	0	0	1205

*Total of lymphocytes counted from a each 32,500 μ^2 field area (six fields were observed from each case).
**Group selection according to degree of glomerular and tubulointerstitial inflammatory cell infiltration and interstitial fibrosis
NA = not available

Table XV. Average number of T-lymphocytes (per 32,500µm^2 field) observed by histopathological group

Data under observation	Degree of glomerular and tubulointerstitial inflammatory cell infiltration and interstitial fibrosis			
	Control/Normal	Mild	Moderate	Severe
Cases per group	3	3	4	4
$CD4^+$	0	0.6	1.5	2.7
$CD8^+$	0	1.0	1.2	4.5
Serum creatinine concentration (µmol/L)	NA	385	676*	724

*Average estimated on three cases only.
NA = not available

Table XVI. Average number of T-lymphocytes (per 32,500μm^2 field) obtained after transformation** for statistical analysis (mean ± 1 SD).

Data under observation	Degree of glomerular and tubulointerstitial inflammatory cell infiltration and interstitial fibrosis			
	Control/Normal	Mild	Moderate	Severe
Cases per group	3	3	4	4
$CD4^+$	0.70±0.00	0.98±0.07	1.22±0.44	1.61±0.50
$CD8^+$	0.70±0.00	1.07±0.20	1.20±0.49	1.84±1.12
($CD4^+$ and $CD8^+$)***	0.70±0.00	1.03±0.14	1.21±0.43	1.73±.81
Serum creatinine concentration (μmol/L)	N/A	385	676*	724

*Average estimated on three cases only.
**Addition of 0.5 to each number obtained from field and followed by square rooting.
***Average number of $CD4^+$ and $CD8^+$

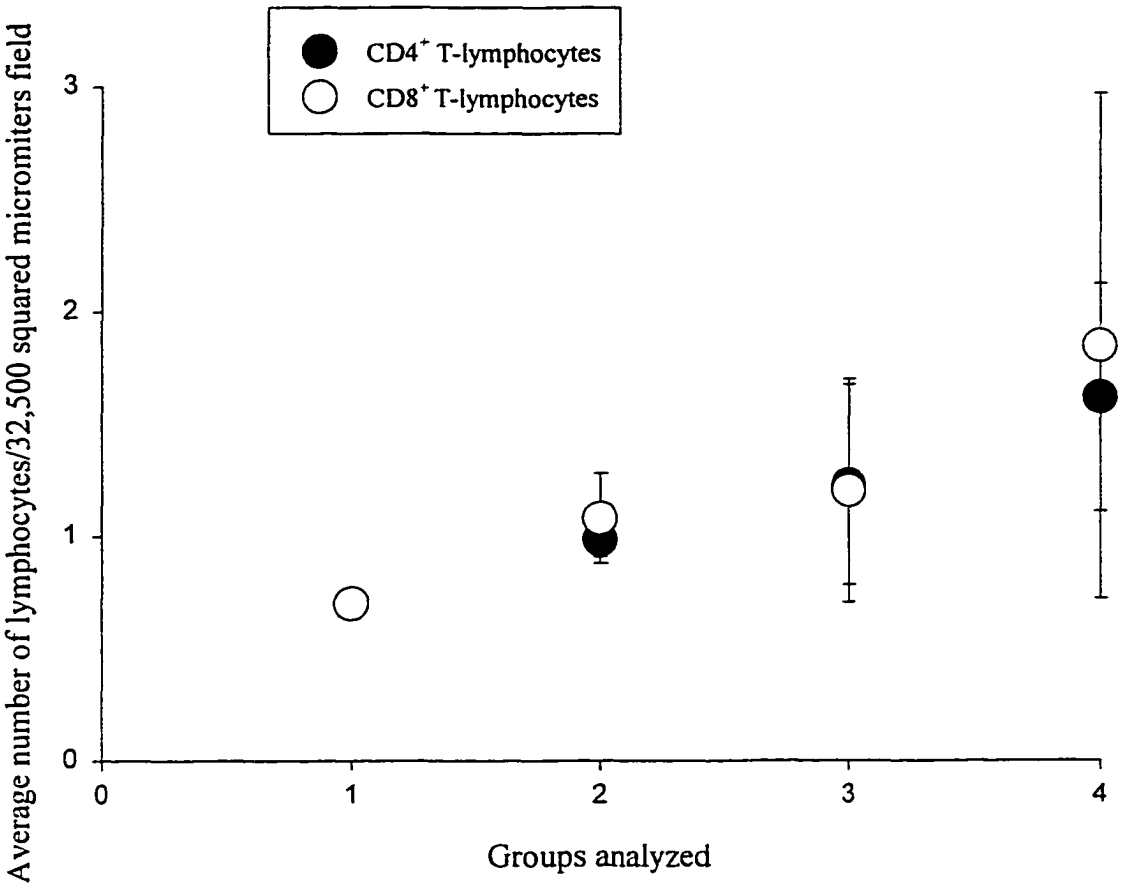

Figure 23. Comparison of the average number of $CD4^+$ and $CD8^+$ T-lymphocytes per goup (using transformed data). Groups identified according to the degree of glomerular and tubulointerstitial inflammatory cell infiltration and interstitial fibrosis: control (1), mild (2), moderate (3), severe (4). Proportion of $CD4^+$ versus $CD8^+$ T-lymphocytes between disease groups was not statistically different.

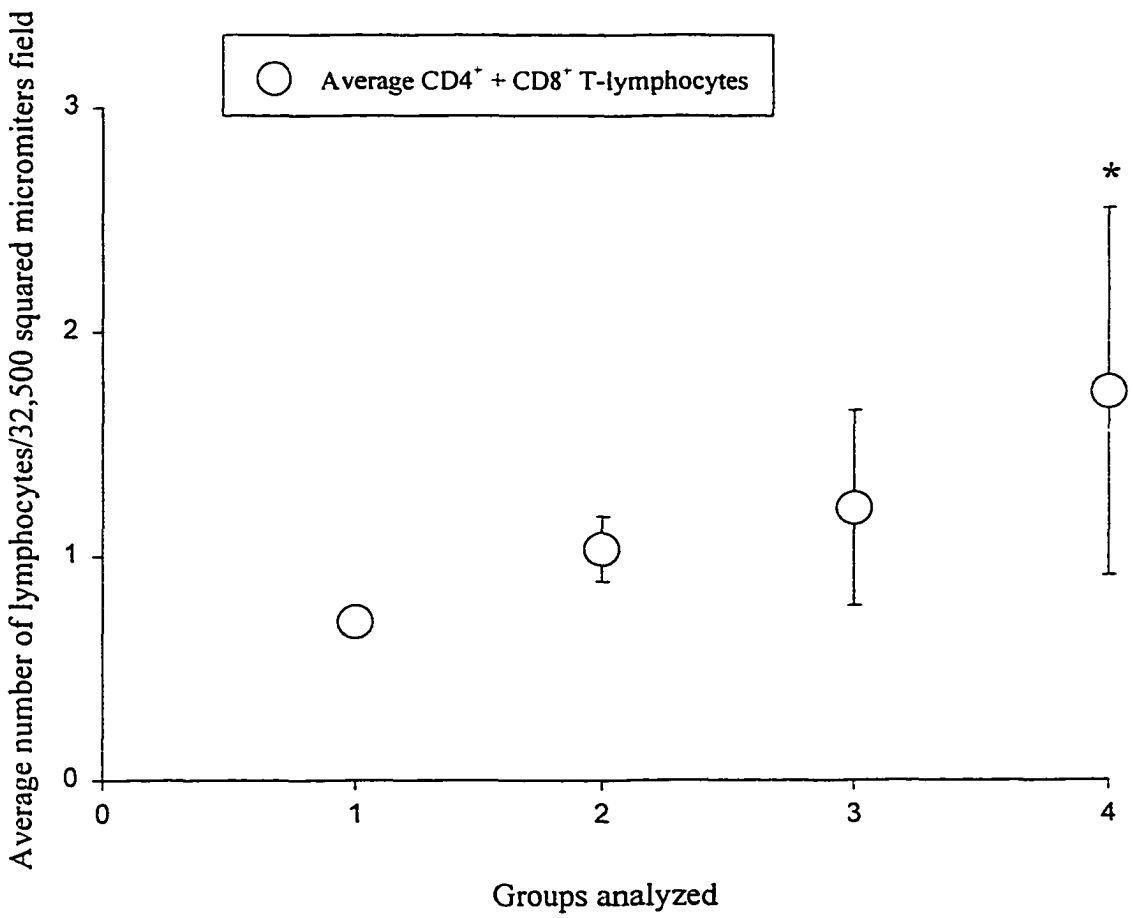

Figure 24. Comparison of the average number of $CD4^+$ plus $CD8^+$ T-lymphocytes per group (using transformed data). Groups identified according to the degree of glomerular and tubulointerstitial inflammatory cell infiltration and interstitial fibrosis: control (1), mild (2), moderate (3), severe (4). Asterisk indicate group that is significantly different than control.

3.4. Discussion

The groups were composed of cases with a histopathological diagnoses of chronic interstitial nephritis, glomerulonephritis, amyloidosis and congenital renal disease. Each disease group had more than one case. Because of limited numbers, the data was not analyzed according to specific renal diseases. Data was analyzed according to histopathological categorization made according to the degree of glomerular and tubulointerstitial inflammatory cell infiltration and interstitial fibrosis. However, the results indicate that regardless of the underlying renal disease, the same proportion of $CD4^+$ and $CD8^+$ T-lymphocytes are present but groups with higher degree of glomerular and tubulointerstitial inflammatory cell infiltration and interstitial fibrosis had a higher number of T-lymphocytes. These findings differ from research in human beings where higher proportion of $CD4^+$ lymphocytes were found (56).

In order for an immune response targeted to tubulointerstitial antigens to be initiated, the antigen must be expressed within the tubulointerstitium of the kidney. T-lymphocytes are present within the tubulointerstitium as a natural cell-mediated host immune response and proliferate in response to antigens. T cells have receptors that recognize peptide fragments transported to the cell surface by specialized molecules of the major histocompatibility complex (MHC) (57). Antigens derived from pathogens that multiply in the cytosol are carried to the cell surface by MHC class I molecules and recognized by $CD8^+$ cytotoxic T cells that will kill the infected cell. Antigens derived from ingested extracellular bacteria and toxins, are carried to the cell surface by MHC class II molecules and recognized by $CD4^+$ T-lymphocytes (58). $CD8^+$ T-cells function in the killing of the target cell and $CD4^+$ T-cells

activate cells bearing specific antigens. T-lymphocyte effector functions are mediated in part by cytokines, which are released when antigen is recognized.

$CD4^+$ and $CD8^+$ T-lymphocytes were present in the canine renal interstitium as a adaptive immune response to a unknown antigen. Additionally, some chemokines (cell surface proteins that are synthesized by macrophages, endothelial cells and fibroblasts) help direct the emigration of inflammatory T-lymphocytes into the interstitium (59). Studies indicate that chemokines, via chemoattractant function, influence interstitial lymphocyte accumulation and modulate the activity of resident renal and inflammatory cells (60). In our study, the groups with a higher degree of glomerular and tubulointerstitial inflammatory cell infiltration and interstitial fibrosis had a higher number of $CD4^+$ and $CD8^+$ T-lymphocytes. However, a multiple comparison on the total number of $CD4^+$ and $CD8^+$ T-lymphocytes between groups showed that only the control group and severe group were statistically different.

The proportion of $CD4^+$ versus $CD8^+$ T-lymphocytes in normal dogs and in dogs with renal disease differs from reports in human beings. Normal kidney tissue from human beings had some T-lymphocyte infiltration (36). In this study, normal canine renal tissue had no T-lymphocyte infiltration. It is possible that the average life-span of a dog is not long enough to expose renal tissue to specific and different antigens compared with the average life-span of humans and this may be is why T-lymphocytes are absent in normal canine renal tissue. The proportions may also differ because exposure to different antigens may elicit different T- lymphocyte responses (additional or different chemokines) in dogs as compared to human beings. It is important to know that $CD4^+$ and $CD8^+$ T-lymphocytes are present in the renal

interstitium because the capacity to modify the movement or function of these cells and their cytokines might provide novel targets for therapeutic interventions (61).

4. GENERAL DISCUSSION

By using morphometrical analysis, an association between glomerular and tubulointerstitial pathologic changes and serum creatinine concentration (used as a measure of renal function) was identified. The number and relative proportion of $CD4^+$ and $CD8^+$ T-lymphocytes in the renal interstitium was determined by using immunohistochemical techniques.

4.1. Association of glomerular and tubulointerstitial pathology and serum creatinine concentration

The present study quantified eleven morphological alterations observed in renal cortical tissue from dogs with naturally occurring renal disease. Two additional measurements such as the absolute volume of kidney/nephron occupied by interstitium and tubules were calculated from four of the eleven measurements. Chronic interstitial nephritis, glomerulonephritis and amyloidosis were the most common renal diseases studied in our investigation.

Three measurements, interstitial volume fraction, tubular volume fraction (tubular wall plus tubular lumen), and Bowman's capsule harmonic thickness were significantly correlated with serum creatinine concentration. Interstitial volume fraction had the strongest correlation with serum creatinine concentration. Morphometric findings from interstitium and tubules of the 39 cases were better associated with renal function (assessed by serum

creatinine concentration) than were glomerular alterations. These findings are similar to those described in human beings (5,6,31),where a closer correlation was present between tubulointerstitial changes and renal function than between glomerular damage and renal function.

4.1.1. Interstitial, volume fraction and absolute volume

Our data showed that the mean percentage volume of interstitial tissue (interstitial volume fraction) in the renal cortex was 19±3% in dogs without renal disease. Interstitial volume fraction of canine renal tissue is approximately twofold greater than the interstitial volume fraction in normal human beings. Interstitial volume fractions ranged from 40% to 78% in the kidneys of dogs with naturally occurring renal disease which included chronic interstitial nephritis, glomerulonephritis, amyloidosis, nephrocalcinosis, and granulomatous nephritis. The absolute volume of interstitium per nephron was significantly increased with increasing creatinine levels. This was not differentially affected by the type of renal disease. Interstitial volume fraction is increased by cellular infiltration (inflammatory cells), fluid (edema) and fibrosis (matrix deposition). Cytokines elaborated by circulating cells (monocytes) recruited into the inflammatory site (tubulointerstitium) may activate proliferative and migratory fibrogenic responses in resident interstitial cells (i.e. fibroblast and mononuclear cells). Activated macrophages play a principal role in fibrogenesis (62) by releasing growth factors such as platelet-derived growth factor (PDGF), a potent chemoatractant for fibroblasts, and transforming growth factor-beta (TGF-β), a strong stimulant for fibroblast proliferation. T-lymphocytes recruited into the site of inflammation

release growth factors which can also stimulate fibroblast proliferation (63).

Interstitial volume fraction was significantly correlated ($r=0.58$, $p<0.05$) with increased serum creatinine concentration. Alterations in interstitial structure can contribute to a tubular and intertubular capillary damage. Interstitial damage can contribute to the reduction in renal function by decreasing the total area of intertubular vessels (10)(decrease filtration due to decreased blood flow). Interstitial inflammation and fibrosis may also occlude the tubules and cause increased intratubular pressure (52). Increased hydrostatic pressure in tubules results in increased Bowman's space pressure which decreases filtration pressure. This may lead to diminished glomerular blood flow, and filtration rate which would result in increased serum creatinine concentration (10).

4.1.2. Tubules, volume fraction and absolute volume

Our data showed that the mean percentage volume of tubules in the renal cortex was 73±4% in dogs without renal disease. A decrease in the mean percentage of tubular volume fractions from 73% to 51-17% were observed in the specimens from dogs with naturally occurring renal disease. The mean percentage volume fraction of tubules decreased significantly ($P<0.05$) in dogs with histopathological diagnoses of chronic interstitial nephritis, glomerulonephritis, amyloidosis and granulomatous nephritis. The serum creatinine concentration was significantly increased when the tubule volume fraction was decreased, with a correlation coefficient (r) of $r=-0.56$, $P<0.05$. The absolute volume of tubules associated with one nephron was not significantly affected by either disease state or serum creatinine concentration (e.g., functional nephrons had tubules which were

morphometrically normal). It is possible that the absolute volume of tubule per nephron does not change because if tubules are present, either functional or regenerating, their volume is maintained.

4.1.3. Bowman's capsule harmonic thickness

In the current study, the average Bowman's capsule thickness was 2.09±0.2 microns in dogs without renal disease. A significant increase in Bowman's capsule thickness (4.89±1.66μ, P=0.004) was observed in dogs with glomerulonephritis. Capsule thickness could increase due to the proliferation of Bowman's capsule cells and/or fibrous thickening of the capsule occurs (19). For the other disease groups, because they were not specific glomerular diseases, Bowman's capsule harmonic thickness was not significantly increased. In addition, Bowman's capsule harmonic thickness was positively and significantly correlated with serum creatinine concentration.

4.1.4. Glomerular area

Glomerular area (μm^2) showed a significant tendency to increase with higher serum creatinine concentration regardless of the renal disease. Moreover, because significant changes were not observed in glomerular tuft area (shrinking), the glomerular area increase was due to an increase in Bowman's space area. The later may be due to increased hydrostatic pressure due to tubular compression by fibrosis and increased Bowman's capsule harmonic thickness. Glomerular area was considered to be the most reliable glomerular measurement to use for the regression analysis because glomerular tuft area, Bowman's

space area, and Bowman's capsule harmonic thickness are included in this measurement.

4.1.4. Regression equation

To observe the effect of each renal measurement (independent variable) on renal function (serum creatinine-dependent variable), a multiple regression analysis was performed on every combination of the independent variables. Based on the highest multiple correlation coefficient (r^2=48.2%, r=0.69, P<0.05) and on the most reliable glomerular measurement, the best measurement to be included in the multiple regression model were interstitium volume fraction ($intV_V$) and glomerular area (glomA). Although, glomerular area had lower correlation coefficient (r=0.40, p=0.01) in comparison to other glomerular measurements, such as Bowman's space area (r=0.51, P=0.01), and Bowman's capsule harmonic thickness (r=0.45, P=0.004), it was considered the most reliable glomerular measurement. To assess which independent variable (i.e. interstitial volume fraction or glomerular area) contributed the most to the variation in serum creatinine concentration (dependent variable), the regression was done on standardized data. The standardized multiple regression equation demonstrated that interstitial volume fraction had a greater (higher number in front of the variable) negative impact on renal function as compared to glomerular area [serum creatinine concentration= 358 + 184 intVV + 122 glomA].

4.2. $CD4^+$ and $CD8^+$ T-lymphocytes in the renal interstitium

Immunohistochemical evaluation of renal tissue revealed that kidney tissue from dogs without renal disease had no T-lymphocyte infiltrates. Renal tissue with different degrees

of glomerular and tubulointerstitial inflammatory cell infiltration and interstitial fibrosis showed $CD4^+$ and $CD8^+$ T-lymphocyte infiltration. Although the number of cases in each subgroup was limited, our results reveal that groups with a higher degree of glomerular and tubulointerstitial inflammatory cell infiltration and interstitial fibrosis had a higher number of $CD4^+$ and $CD8^+$ T-lymphocytes. However, the severe group was the only group with a statistically significant (P=0.007) higher number of $CD4^+$ and $CD8^+$ T-lymphocytes compared to the control group. Also, $CD4^+$ cells were present in the same proportion as $CD8^+$ cells in mild, moderate and severe groups. However in a few cases, $CD8^+$ lymphocytes were more numerous (case one and three from severe group) or they were not present (case two and three from moderate, and case two from severe group).

The migration of leukocytes from the circulation into the renal interstitium is associated with a complex immune response. Both the stage of the immune response and the type of tissue response determine which of the subsets (e.g. lymphocytes, polymorphonuclear leukocytes, macrophages) of leukocytes will comprise the inflammatory cell infiltrates (60). In addition, these infiltrates are, in large part, determined by the activity of multiple interaction molecules (e.g., cytokines, complement C5a)(60). A superfamily of interaction molecules (chemokines) are synthesized and secreted by renal cells, such as mesangial cells, endothelial cells, and tubular cells and they can activate $CD4^+$ and $CD8^+$ T-lymphocytes (60). This could be one possible mechanism to explain the presence of the ($CD4^+$ and $CD8^+$) T-lymphocytes in diseased kidneys of dogs.

4.3. Conclusion

The present study revealed that significant structural alterations are present in the cortex of dogs with naturally occurring chronic interstitial nephritis, glomerulonephritis, amyloidosis, nephrocalcinosis and granulomatous nephritis. The alterations were increased interstitial absolute volume per nephron and interstitial volume fraction, decreased tubular volume fraction but unchanged absolute volume of tubule per nephron and increased Bowman's capsule thickness. A statistically positive correlation exists between serum creatinine concentration and interstitial volume fraction, tubular volume fraction, glomerular area, Bowman's space area, Bowman's capsule thickness and volume weighted mean volume of the glomerulus. Interstitial volume fraction and absolute interstitial volume per nephron are strongly associated with serum creatinine concentration as opposed to glomerular abnormalities.

T-lymphocyte subsets ($CD4^+$ and $CD8^+$) are present within the renal interstitium of dogs with naturally occurring renal disease. The proportion of $CD4^+$ versus $CD8^+$ T-lymphocytes is similar in the kidney of dogs with naturally occurring renal disease in this study. The number of $CD4^+$ and $CD8^+$ T-lymphocytes increases with the severity of histopathological renal lesions.

REFERENCES

1. POLZIN DJ, OSBORNE CA, BARTGES JW, ET AL. Chronic Renal Failure. Ettinger SJ and Feldman EC, Eds. In: Textbook of Veterinary Internal Medicine. 4th ed. Philadelphia, PA: W.B. Saunders, 1995; 134, pp. 1734-1760.

2. GRAUER GF, DIBARTOLA SP. Glomerular Disease. Ettinger SJ and Feldman EC, Eds. In: Textbook of Veterinary Internal Medicine. 4th ed. Philadelphia, PA: W.B. Saunders, 1995; 135, pp. 1760-1775.

3. BENNETT WM, ELZINGA LW, PORTER GA. Tubulointerstitial Disease and Toxic Nephropathy. Brenner BM and Rector FC, Eds. In: The Kidney. 4th ed. Philadelphia, PA: W.B. Saunders, 1991; 29, pp. 1430-1496.

4. OKADA H., STRUTZ F., DANOFF T.M., KALLURI R., NEILSON E.G. Possible mechanisms of renal fibrosis. Contrib Nephrol. 1996; 118:147-154.

5. MACKENSEN-HAEN S., BADER R., GRUND K.E., BOHLE A. Correlations between renal cortical interstitial fibrosis, atrophy of the proximal tubules and impairment of the glomerular filtration rate. Clin Nephrol. 1981; 15:167-171.

6. BOHLE A., MACKENSEN-HAEN S., VON GISE H. Significance of tubulointerstitial changes in the renal cortex for the excretory function and concentration ability of the kidney: a morphometric contribution. Am J Nephrol. 1987; 7:421-433.

7. ABE S., AMAGASAKI Y., IYORI S., KONISHI K., KATO E., SAKAGUCHI H. Significance of tubulointerstitial lesions in biopsy specimens of glomerulonephritic patients. Am J Nephrol. 1989; 9:30-37.

8. SCHAINUCK L.I., STRIKER G.E., CUTLER R.E., BENDITT E.P. Structural-functional correlations in renal disease. II. The correlations. Human Pathol. 1970; 1:631-641.

9. BOHLE A., GLOMB D., GRUND K.E., MACKENSEN S. Correlation between relative interstitial volume of the renal cortex and serum creatinine concentration in minimal changes with nephrotic syndrome and in focal sclerosing glomerulonephritis. Virchows Arch A Path Anat and Histol. 1977; 376:221-232.

10. BOHLE A., BADER R., GRUND K.E., MACKENSEN S., NEUNHOEFFER. Serum creatinine concentration and renal interstitial volume. Analysis of correlations in endocapillary (acute) glomerulonephritis and in moderately severe mesangioproliferative glomerulonephritis. Virchows Arch A Path Anat and Histol. 1977; 375:87-96.

11. KUNCIO G.S., NEILSON E.G., HAVERTY T. Mechanisms of tubulointerstitial fibrosis. Kidney Int. 1991; 39:550-556.

12. BERTRAM J.F. Analyzing renal glomeruli with the new stereology. Int Rev Cytol. 1995; 161:111-172.

13. WEIBEL ER. Introduction. Weibel ER, Ed. In: Stereological Methods. San Diego, CA: Academic Press, 1979; 1, pp. 1-8.

14. NIKOLIC PATERSON D.J., LAN H.Y., HILL P.A., ATKINS R.C. Macrophages in renal injury. Kidney Int Suppl. 1994; 45:S79-82.

15. STRUTZ F., NEILSON E.G. The role of lymphocytes in the progression of interstitial disease. Kidney Int Suppl. 1994; 45:S106-10.

16. DENTON K.M., FENNESSY P.A., ALCORN D., ANDERSON W.P. Morphometric analysis of the actions of angiotensin II on renal arterioles and glomeruli. Am J Physiol. 1992; 262:F367-72.

17. RUCKEBUSCH Y, PHANEUF L, DUNLOP R. Renal acid-base balance. Ruckebusch Y, Phaneuf L and Dunlop R, Eds. In: Physiology of Small and Large Animals. Philadelphia, PA: B.C. Decker Inc. 1991; 18, pp. 167-173.

18. BERTRAM J.F., SOOSAIPILLAI M.C., RICARDO S.D., RYAN G.B. Total numbers of glomeruli and individual glomerular cell types in the normal rat kidney. Cell Tissue Res. 1992; 270:37-45.

19. TISHER CC, MADSEN KM. Anatomy of the Kidney. Brenner BM and Rector FC, Eds. In: The Kidney. 4th ed. Philadelphia, PA: W.B.Saunders Company, 1991; 1, pp. 60-65.

20. OSBORNE CA, FLETCHER TF. Applied Anatomy of the Urinary System with Clinicopathologic Correlation. Osborne CA and Finco DR, Eds. In: Canine and Feline Nephrology and Urology. Media, PA: Williams & Wilkins, 1995; 1, pp. 3-28.

21. CONFER AW, PANCIERA RJ. The Urinary System. Carlton WW and McGavin MD, Eds. In: Special Veterinary Pathology. 2nd ed. St. Louis, M. Mosby-Year Book, 1995; 5, pp. 209-246.

22. RUCKEBUSCH Y, PHANEUF L, DUNLOP R. The Urinary System. Ruckebusch Y, Phaneuf L and Dunlop R, Eds. In: Physiology of Small and Large Animals. Philadelphia, PA: B.C. Decker Inc. 1991; 15, pp. 146-151.

23. DUNNILL M.S., HALLEY W. Some observations on the quantitative anatomy of the kidney. J Pathol. 1973; 110:113-121.

24. LEMLEY K.V., KRIZ W. Anatomy of the renal interstitium. Kidney Int. 1991; 39:370-381.

25. WOLF G., NEILSON E.G. Cellular biology of tubulointerstitial growth. Curr Top Pathol. 1995; 88:69-97.

26. MACKENSEN S., GRUND K.E., SINDJIC M., BOHLE A. Influence of the renal cortical interstitium on the serum creatinine concentration and serum creatinine clearance in different chronic sclerosing interstitial nephritides. Nephron. 1979; 24:30-34.

27. BOHLE A., MACKENSEN HAEN S., WEHRMANN M. Significance of postglomerular capillaries in the pathogenesis of chronic renal failure. Kidney Blood Press Res. 1996; 19:191-195.

28. BOHLE A., GRUND K.E., MACKENSEN S., TOLON M. Correlations between renal interstitium and level of serum creatinine. Morphometric investigations of biopsies in perimembranous glomerulonephritis. Virchows Arch A Pathol Pathol Anat. 1977; 373:15-22.

29. FISCHBACH H., MACKENSEN S., GRUND K.E., KELLNER A., BOHLE A. Relationship between glomerular lesions, serum creatinine and interstitial volume in membrano-proliferative glomerulonephritis. Klin Wochenschr. 1977; 55:603-608.

30. MACKENSEN S., GRUND K.E., BADER R., BOHLE A. The influence of glomerular and interstitial factors on the serum creatinine concentration in renal amyloidosis. Virchows Arch A Path Anat and Histol. 1977; 375:159-168.

31. BOHLE A., VON GISE H., MACKENSEN-HAEN S., STARK-JAKOB B. The obliteration of the postglomerular capillaries and its influence upon the function of both glomeruli and tubuli. Functional interpretation of morphologic findings. Klin Wochenschr. 1981; 59:1043-1051.

32. MACKENSEN HAEN S., BOHLE A., CHRISTENSEN J., WEHRMANN M., KENDZIORRA H., KOKOT F. The consequences for renal function of widening of the interstitium and changes in the tubular epithelium of the renal cortex and outer medulla in various renal diseases. Clin Nephrol. 1992; 37:70-77.

33. JULES ME. Immunohistochemical Methods. Borysewicz S and Elias R, Eds. In: Immunohistopathology a practical approach to diagnosis. Chicago: American Society of Clinical Pathologists, 1990; 1, pp. 1-90.

34. HAINES D.M., CHELACK B.J. Technical considerations for developing enzyme immunohistochemical staining procedures on formalin-fixed paraffin-embedded tissues for diagnostic pathology. J Vet Diagn Invest. 1991; 3:101-112.

35. BOENISCH T, FARMILO AJ, STEAD R. Immunochemical staining methods. California. DAKO Corporation. 1989.

36. HOOKE D.H., GEE D.C., ATKINS R.C. Leukocyte analysis using monoclonal antibodies in human glomerulonephritis. Kidney Int. 1987; 31:964-972.

37. MAIN I.W., NIKOLIC PATERSON D.J., ATKINS R.C. T cells and macrophages and their role in renal injury. Semin Nephrol. 1992; 12:395-407.

38. PRODJOSUDJADI W., GERRITSMA J.S., VAN ES L.A., DAHA M.R., BRUIJN J.A. Monocyte chemoattractant protein-1 in normal and diseased human kidneys: an immunohistochemical analysis. Clin Nephrol. 1995; 44:148-155.

39. TRUONG L.D., FARHOOD A., TASBY J., GILLUM D. Experimental chronic renal ischemia: morphologic and immunologic studies. Kidney Int. 1992; 41:1676-1689.

40. MAMPASO F.M., WILSON C.B. Characterization of inflammatory cells in autoimmune tubulointerstitial nephritis in rats. Kidney Int. 1983; 23:448-457.

41. HAVERTY T.P., KELLY C.J., HOYER J.R., ALVAREZ R., NEILSON E.G. Tubular antigen-binding proteins repress transcription of type IV collagen in the autoimmune target epithelium of experimental interstitial nephritis. J Clin Invest. 1992; 89:517-523.

42. EDDY A.A. Interstitial nephritis induced by protein-overload proteinuria. Am J Pathol. 1989; 135:719-733.

43. YEE J., KUNCIO G.S., NEILSON E.G. Tubulointerstitial injury following glomerulonephritis. Semin Nephrol. 1991; 11:361-366.

44. ROSE BD. Introduction to renal function. Rose BD, Ed. In: Clinical Physiology of Acid-base and Electrolyte Disorder. 4th ed. New York: McGraw-Hill, Inc. 1998; 1, pp. 3-19.

45. BORDER W.A., OKUDA S., NAKAMURA T., LANGUINO L.R., RUOSLAHTI E. Role of TGF-beta 1 in experimental glomerulonephritis. Ciba Found Symp. 1991; 157:178-189.

46. ROSE BD. Renal Circulation and Glomerular Filtration Rate. Burton DR, Ed. In: Clinical Physiology of Acid-Base and Electrolyte Disorders. 4th ed. McGraw-Hill, Inc. 1994; 2, pp. 20-65.

47. WEIBEL ER. Point counting methods. Weibel ER, Ed. In: Stereological Methods. San Diego, CA: Academic Press, 1979; 4, pp. 101-161.

48. WEIBEL ER. Various methods. Weibel ER, Ed. In: Stereological Methods. San Diego, CA: Academic Press, 1979; 6, pp. 204-236.

49. GUNDERSEN H.J., JENSEN E.B. Stereological estimation of the volume-weighted mean volume of arbitrary particles observed on random sections. J Microsc. 1985; 138:127-142.

50. Methods for Carbohydrates and Mucoproteins. Luna LG, Ed. 3rd ed. USA: McGraw-Hill, 1968; 10, pp. 153-173.

51. BAUMBACH L., SKOTT O. Renin release from different parts of rat afferent arterioles in vitro. Am J Physiol. 1986; 251:F12-6.

52. KELLY CJ, NEILSON EG. Tubulointerstitial Disease. Brenner BM, Ed. In: The Kidney. 5th ed. Philadelphia, PA: W.B. Saunders Company, 1996; 33, pp. 1655-1679.

53. KELLEY V.R., DIAZ-GALLO C., JEVNIKAR A.M., SINGER G.G. Renal tubular epithelial and T cell interactions in autoimmune renal disease. Kidney Int Suppl. 1993; 39:S108-15.

54. TAYLOR CR, SHI SR. Fixation, Processing, Special Application. Taylor CR and Cote RJ, Eds. In: Immunomicroscopy: A Diagnostic Tool for the Surgical Pathologist. 2nd ed. Philadelphia, PA: W.B. Saunders Company, 1994; 3, pp. 42-70.

55. STEEL RGD, TORRIE JH. Analysis of variance II: Multiway classifications. Napier C and Maisel JW, Eds. In: Principles and Procedures of Statistics a Biomedical Approach. 2nd ed. New York: McGraw-Hill, Inc. 1980; 9, pp. 195-238.

56. ALEXOPOULOS E., SERON D., HARTLEY R.B., CAMERON J.S. Lupus nephritis: correlation of interstitial cells with glomerular function. Kidney Int. 1990; 37:100-109.

57. JANEWAY CA, TRAVERS P. Basic Concepts in Immunology. Robertson M, Ed. In: Immunobiology: The immune system in health and disease. London/New York: Current Biology Ltd/Garland Publishing Inc, 1994; 1, pp. 1-43.

58. JANEWAY CA, TRAVERS P. T-Cell Mediated Immunity. Robertson M, Ed. In: Immunobiology: Thr immune system in health and disease. London New York: Current Biology Ltd/Publishing Inc, 1994; 7, pp. 7-49.

59. DANOFF T.M. Chemokines in interstitial injury [editorial; comment]. Kidney Int. 1998; 53:1807-1808.

60. DANOFF TM, NEILSON EG. The Role of Chemoattractants in Renal Disease. Neilson EG and Couser WG, Eds. In: Immunologic Renal Disease. Philadelphia, PA: Lippincott-Raven, 1998; 24, pp. 499-517.

61. LUSTER A.D. Chemokines--chemotactic cytokines that mediate inflammation. N Engl J Med. 1998; 338:436-445.

62. WAHL S.M. Host immune factors regulating fibrosis. Ciba Found Symp. 1985; 114:175-195.

63. NIELSON E.G., PHILLIPS S.M., JIMENEZ S. Lymphokine modulation of fibroblast proliferation. J Immunol. 1982; 128:1484-1486.

IMAGE EVALUATION TEST TARGET (QA-3)

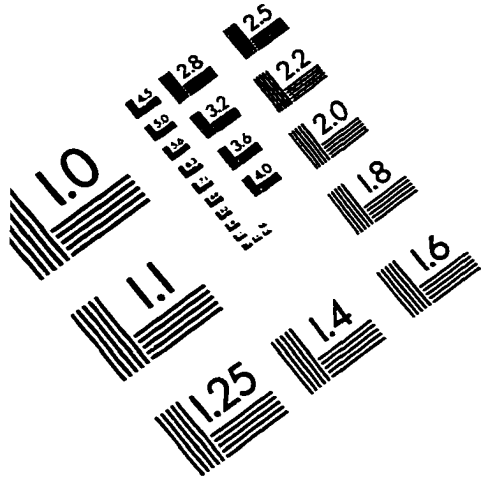

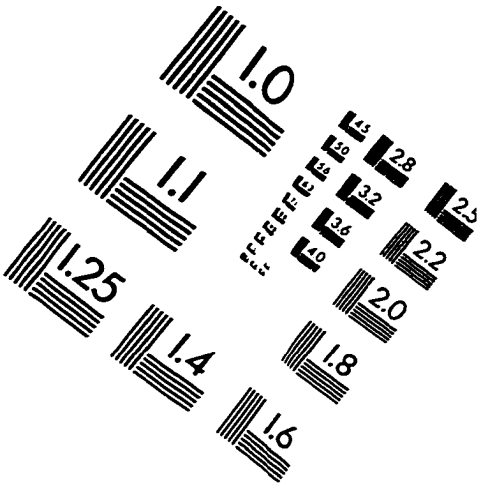

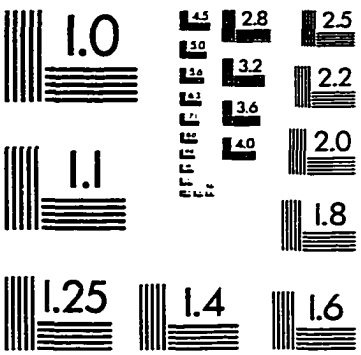

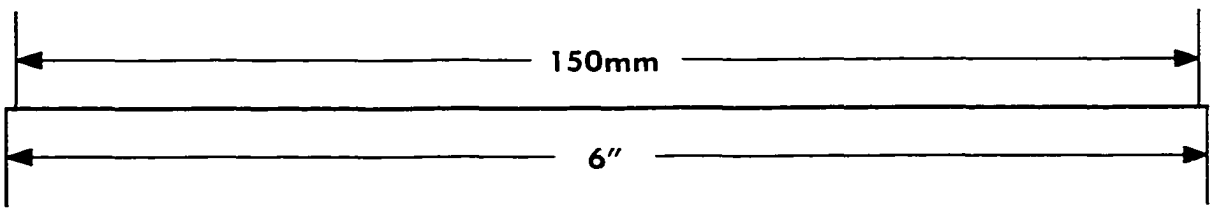

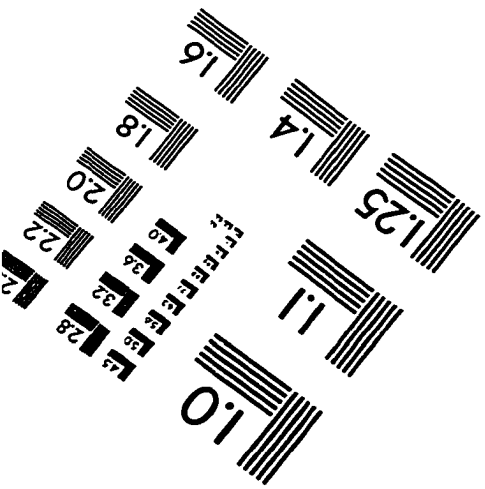

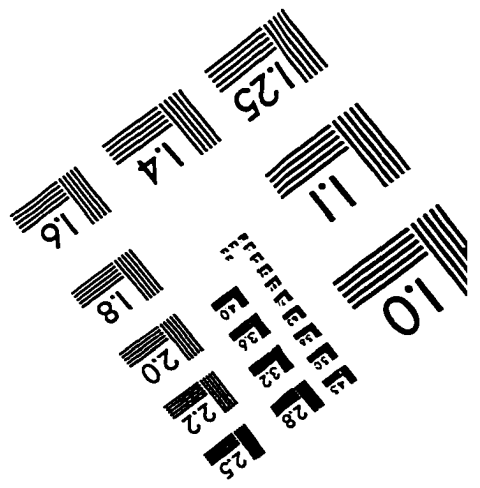

APPLIED IMAGE, Inc
1653 East Main Street
Rochester, NY 14609 USA
Phone: 716/482-0300
Fax: 716/288-5989